Copy 6
RM E56B10

NACA RM E56B10

NACA

RESEARCH MEMORANDUM

ANALYSIS OF A FORM OF PEAK HOLDING CONTROL

By G. J. Delio

Lewis Flight Propulsion Laboratory
Cleveland, Ohio

NATIONAL ADVISORY COMMITTEE
FOR AERONAUTICS

WASHINGTON

March 30, 1956

NACA RM E56B10

NATIONAL ADVISORY COMMITTEE FOR AERONAUTICS

RESEARCH MEMORANDUM

ANALYSIS OF A FORM OF PEAK HOLDING CONTROL

By G. J. Delio

SUMMARY

A typical plant process was studied in which the output increased with the input until a definite maximum was reached. Beyond that maximum, a sudden drop with an associated inert zone occurred in the output. Turbojet-engine operation in the vicinity of stalled compressor performance is a process of this type and was considered in detail.

The output, as it varied about its maximum value, was subjected to harmonic analysis to determine signal possibilities, and the results were used in the design of the control. A band-pass filter selected a particular harmonic function and used it in a prescribed manner as negative feedback to maintain the input that produced maximum average output.

This form of peak holding control, which is one method of obtaining information from a peak output for purposes of maintaining that peak, was studied for the following criteria: maintenance of maximum peak average output, minimum duration beyond peak output, quickness in response to reach peak condition, and type of stability.

The control investigated maintained an average output less than that realizable when the input was at the maximum value. The average output was directly related to the perturbation amplitude, the magnitude of drop occurring at the peak, and the width of the inert zone in the input. It also depended on the center frequency and band width of the band-pass filter used to measure harmonic content.

INTRODUCTION

There are certain processes in which the plant output increases to a definite maximum as the input is increased. A further increase in the input is followed by a sudden drop in the output to a value that may be uneconomical and perhaps damaging. These processes are found in various forms: mechanical, chemical, hydrodynamic, electrical, magnetic, and so forth. The need for obtaining the maximum output from these plants presents a problem in control, and the control of the described plant process leads to a study of a form of peak holding control.

Most controls try to maintain the output either constant or at a prescribed change using error data (difference between desired output and measured output) supplied continuously in an uninterrupted flow. This study is concerned with peak holding control of the described process. The control is actuated by error data supplied intermittently and not necessarily at discrete moments equally spaced in time. The output is sampled periodically, and the average input that causes the output to be near its maximum value is maintained.

An example of the described plant process is the acceleration of gas-turbine engines. Compressor-discharge pressure increases with increasing fuel flow and reaches a maximum as compressor stall is approached. At stall, the pressure suddenly drops. Because of the relation between pressure increase and accelerating torque, a control that maintains maximum pressure increase would also maintain maximum acceleration, or nearly so.

A control of this process may be obtained by superimposing a perturbation on the input fuel flow to determine the proximity of stall. The control would increase the average fuel flow toward the maximum and probe for the maximum pressure at the perturbation frequency until the sudden drop in output pressure is sampled. The drop into the undesirable region of operation would determine the desired maximum fuel flow and corresponding maximum pressure ratio across the compressor.

In order to facilitate the study of peak holding control, a function generator was synthesized that simulated the essential features of a turbojet-engine compressor, in particular, the pressure drop and hysteresis at stall. Then a control was designed that selected the information from the simulator output that characterized the peak output and used it in a manner prescribed to cause the simulator output to reach and remain near its maximum average value. Both the simulator and control were composed of units of an electronic differential analyzer.

The general objective of this report is a study of the characteristics of the described form of peak holding control. The control has not yet been used in experimental turbojet-engine study. This study is concerned with only one method of extracting the maximum amount of information from a peak output for the purpose of maintaining that peak. The criteria sought in this control process are: maintenance of peak average output, minimum duration of time in undesirable operation, quickness in response to command to reach peak condition, least amount of excursion in the undesirable region, and type of stability.

[redacted]

PROCEDURE

The investigation of control possibilities was performed by first determining an idealized compressor function from a study of experimental pressure responses in the vicinity of the stall region. Then signal possibilities were sought by performing a harmonic analysis on the pressure output. The results of this harmonic analysis were used as a guide in a control design. The control was applied to the simulator, and an analysis of control behavior was made.

Analysis

The compressor function was determined by a study of pressure response and acceleration resulting from fuel-flow changes at constant-speed conditions. When the input fuel flow (with a superimposed perturbation) is near the value corresponding to a maximum output, the resulting sudden pressure drop causes the output to be rich in harmonics. A Fourier analysis of the pressure output in this region was used as a guide in the selection of usable information for control synthesis.

Determination of compressor function. - As shown in figure 1(a), the compressor-discharge pressure drops suddenly when the critical-pressure ratio is reached at stall. The speed shows an instantaneous change in acceleration. Both changes indicate stalled turbojet behavior. Their value at the time of stall represents the peak values to be maintained.

From this type of data, the plots of figures 1(b) and (c) were made. Both the pressure change and acceleration, at constant-speed conditions, increase with fuel flow. The increase becomes less as the fuel flow reaches the value sufficient to cause stall. At stall, both the compressor-discharge pressure and acceleration decrease. The decreasing radius of curvature shown on these figures indicates that harmonic content in the output should increase as the peak value is reached.

If the high-frequency fluctuation during stall is ignored and average pressure is substituted (fig. 1(a)), if the pressure gain with respect to fuel flow (at constant speed) is assumed linear and to possess the same slope throughout the speed range (fig. 1(b)), if surge behavior is neglected, and if arbitrary values are used for an inert zone in the fuel-flow input, then the idealized function shown in figure 1(d) results.

This function describes an input fuel-flow level $\overline{w}_f$ that produces a linear output pressure increase ΔP at slope m until the stall value $\overline{\Delta P}$ is reached. At this point there is an instantaneous pressure

drop Δp. (Symbols are defined in appendix A.) For the case with an inert zone in fuel flow, the output follows the path indicated. Thus the combination of the inert zone in fuel flow and the pressure drop describes a hysteresis loop.

The idealized function defined for the cases with and without hysteresis describes a plant process that should serve as a rigid test for peak holding control. The constant slope up to the maximum value contains no information that could warn of the impending sudden drop. The sudden drop in the output must be sampled for this control to determine the maximum value $\overline{\Delta P}$. On the other hand, if the slope decreased with increasing input (fig. 1(b)), the control could hold at some minimum positive slope without the need for sampling the sudden pressure drop.

The size of the inert zone indicated in figure 1(d) is arbitrary. Its magnitude has not been definitely established. It could be relatively small if the input were checked at the instant stall is sensed, thus minimizing the amount of excess fuel dumped into the combustors. This excess, representing delayed combustion, would maintain the output pressure after the controlled input fuel flow had been reduced. If fuel flow were checked at the value producing maximum pressure, the only contribution to hysteresis could be from aerodynamic considerations and there would be none from the combustion process.

Signal possibilities. - If, for mathematical convenience, a test signal $A \sin \omega_0 t$ is superimposed on the input fuel-flow level when the input level is well below $\overline{\Delta w_f}$, the output will contain the fundamental frequency in undistorted form. When the average fuel flow is near $\overline{\Delta w_f}$, the output pressure ΔP will be distorted, as indicated in figure 1(d). Assuming that the output $f(t)$ is periodic, a Fourier series of the form

$$f(t) = \frac{a_0}{2} + \sum_{n=1}^{\infty} a_n \cos nt + \sum_{n=1}^{\infty} b_n \sin nt$$

may be developed. Now assuming that for small excursions into the undesirable region the output depends on the parallel slope $N = \text{constant}$, the Fourier analysis of the output yields

With hysteresis:

$$f(t) = \left[\overline{mw}_f - \frac{\Delta p}{2\pi}(\varphi_1 - \varphi_2)\right] + \left[ma + \frac{\Delta p}{\pi}(\cos \varphi_2 - \cos \varphi_1)\right] \sin \varphi +$$

$$\frac{\Delta p}{\pi} \sum_{n=2}^{\infty} \left[(\cos n\varphi_2 - \cos n\varphi_1) \frac{\sin n\varphi}{n} - (\sin n\varphi_2 - \sin n\varphi_1) \frac{\cos n\varphi}{n}\right]$$

[redacted]

where

$\varphi_1 = \omega_0 t_1$ stall inception angle

$\varphi_2 = \omega_0 t_2$ stall recovery angle

No hysteresis:

$$f(t) = \left[\bar{mx} - \frac{\Delta p}{\pi}\left(1 - \frac{4t_1}{T}\right)\right] + \left(ma - \frac{2\Delta p}{\pi}\cos\varphi_1\right)\sin\varphi + \frac{\Delta p}{\pi}\sum_{n=2}^{\infty}\left[(-1^n + 1)\sin n\varphi_1 \frac{\cos n\varphi}{n} + (-1^n - 1)\cos n\varphi_1 \frac{\sin n\varphi}{n}\right]$$

For the case with no hysteresis, the average output pressure for a particular input fuel-flow level $\bar{w}_f$ becomes

$$\tilde{\Delta P} = m\bar{w}_f - \frac{\Delta p}{2}\left(1 - \frac{2\varphi_1}{\pi}\right)$$

But since the maximum output pressure is

$$\bar{\Delta P} = m\bar{w}_f + ma \sin\varphi_1$$

the loss in the average output pressure becomes

$$1 - \frac{\tilde{\Delta P}}{\bar{\Delta P}} = \frac{ma}{\bar{\Delta P}}\sin\varphi_1 + \frac{\Delta p}{\bar{\Delta P}}\left(\frac{\pi - 2\varphi_1}{2\pi}\right)$$

The amplitudes of the various harmonics of $f(t)$ with no hysteresis are plotted in figure 2 as functions of the stall inception angle φ_1, or that instant of the fundamental period when maximum pressure is reached. Figure 2(a) shows that the ratio of average pressure rise to maximum pressure rise $\tilde{\Delta P}/\bar{\Delta P}$ decreases as the increasing average fuel flow probes into the stall region. The maximum amplitudes of the even harmonics decrease with increasing order, and the maximum occurs progressively close to the quarter-period time.

In figure 2(b) the amplitude of the first harmonic starts to decrease at the moment stall is experienced and becomes zero when stall duration is for one-sixth of the period. A control based on this sign reversal could maintain average fuel flow at a value that would cause stall to be experienced during one-sixth of every period with a corresponding loss in average pressure increase. The amplitudes of the remaining odd harmonics become progressively small with increasing order.

The mean-square value of each harmonic (fig. 2(c)) computed from

$$\frac{a_0^2}{4} + \sum_1^n \frac{a_n^2 + b_n^2}{2}$$

decreases with increasing order, and the maximum value for the first harmonic occurs closer to the quarter-period time. When either the odd or even harmonic is at its maximum value, stall duration is for π/n part of the period. Stall inception is at $\frac{\pi}{2}\left(1 - \frac{1}{n}\right)$ part of the period.

The effect of summing the harmonics is illustrated in figure 2(d). The maximum value increases and stall inception approaches the quarter-period time. Thus, a control that used some function of the harmonic content of the output as negative feedback could maintain the input fuel-flow level near its maximum value. The mean-square values of the harmonics bear a ratio to each other, as shown in figure 2(c). A particular choice of harmonics (fig. 2(d)) affects the remaining parameters in a control; that is, the second harmonic is at a maximum when stall is experienced for a quarter cycle of the test frequency, whereas the tenth harmonic would need amplification but would be a maximum when stall is experienced for only a twentieth of a cycle. The corresponding drop in average output pressure, however, would be less.

Method of Control

The idealized function in figure 1(d) was simulated by an amplifier-diode circuit using commercially available components of an electronic differential analyzer. The simulator was then used as a plant process to be controlled. The control used a band-pass filter that selected particular harmonics from the output when stall was experienced and used them as negative feedback to reduce the fuel flow.

Simulation. - The nonlinear characteristics of the compressor function were simulated with the elements shown in figure 3. The first element is a comparator. It compares the input with a reference limit E_3, which is analogous to the maximum value $\overline{\Delta P}$. When the input reaches this value, the comparator output suddenly drops by an amount E_1, which is analogous to the sudden drop Δp following the maximum value.

The comparator serves as an input to a limiter (element 2). This element has unit negative slope and limits its output to E_2 when its input drops below $-E_2$. The value E_2 is analogous to the inert zone in the input. When the limiter output is fed back positively, thus

closing the loop, the comparator output functions as a bistable multivibrator of modified form, provided the input sweeps through a suitable range. It has a hysteresis loop whose position and area are independent functions of the three variable parameters E_1, E_2, and E_3.

The input to the comparator also serves as an input to a limiter with positive unit slope (element 3). Its output is limited at the value of maximum pressure rise E_3. When this output is summed (element 4) with the comparator output, a function generator results that compares closely with the idealized function of figure 1(d). The actual function-generator output is shown in figure 4, and the detailed description of the design is contained in appendix B. The simulator describes an input fuel-flow change e_i (volts) that produces a linear output pressure change e_o (volts) with a slope m until the stall value E_3 is reached. Here the output drops by the amount E_1 (pressure drop) to an average stall value and remains at this value for further increases in e_i. For decreasing e_i, the output follows the path indicated to describe the assumed hysteresis loop.

Method. - A sinusoidal variation in the input, when the input e_i is close to E_3, produces a pulse of duration t and height equal to E_1. If a control could manipulate the input in an effort to minimize the pulse duration, it would maintain the plant process mostly in the desirable region and would yield an average output near the maximum value E_3. The information contained in the pulse must be used as quickly and efficiently as possible.

The frequency spectrum of a pulse is shown in figure 5. Most of the signal power is localized at the low-frequency end. However, for purposes of control, only the increase in the output is of importance. The average output value is not required. The fundamental frequency (fig. 2(b)) presents difficulties in its use in control. Also, the contribution from the frequency range above $1/t$ is negligible. Thus only those frequencies between the second harmonic and $1/t$ are used in control.

One possible control is shown schematically in figure 6(a). The simplified block diagram is shown in figure 6(b). A band-pass filter selects the particular harmonic or group of harmonics from the simulator output. This output is rectified to produce the absolute value $|G(s)|$, which is then amplified by the amount K. The output of the absolute-value device $K|G(s)|$ exists only when the peak value of the simulator E_3 is reached; otherwise, it is zero.

A forcing bias C, whose integral produces a ramp velocity that drives the input toward the maximum value, is summed with the preceding

output. The integral of this sum produces a ramp velocity of C units per τ seconds during the time existing before the peak value E_3 is sampled. When the peak value is reached, the generated signal produces an average absolute value. This value $K|G(s)|$, present only when the peak value is sampled, subtracts from the forcing bias to reduce the ramp velocity. The ramp velocity reduces to zero at the time the amplified average absolute value of the filter output is equal and opposite to the forcing bias. Under this condition the peak value will be held. The integrator output is summed with the perturbation $A \sin \omega_0 t$, and this sum is used as the input to the simulator; thus the loop is closed. The controller output which manipulates the input e_i into the simulator becomes

$$e_i = 20 \int (C - K|G(s)|)dt + A \sin \omega_0 t$$

using the constant given in figure 6(a).

The use of a perfect ideal filter and absolute-value device was assumed with the described theoretical control. The imperfect filter does not completely separate the signal from the noise environment. However, a minimum-width band-pass filter, used in the control, can considerably increase the signal-to-noise ratio. The imperfect filter, because of its selectivity limitations, will also cause deviation from theoretical control behavior. Thus, the entire control depends to a great degree upon filter characteristics.

The filter behavior is described by figure 7(a). The filter is a commercially available unit having essentially linear phase shift in the pass band together with approximately zero-decibel insertion loss. At the minimum band width, the insertion loss is one-half. However, there exist a delay time and build-up time that are inversely proportional to the band width. They depend mainly on the slope of the phase function within the pass band; that is, they increase with selectivity (ref. 1).

Filter responses to input pulses are shown in figure 7(b). The ringing amplitude and time decrease with increasing center frequency (fig. 7(b), left) and increases with band width (fig. 7(b), right). The amplified absolute values are also shown.

For the purposes of control only the higher harmonics generated at the peak are desired. The direct-current and the fundamental harmonic yield only information characterizing the region below the peak value. The left side of figure 7(c) illustrates the cut-off characteristics of the filter. For a center frequency at the second harmonic and minimum band width (the fundamental is chosen at 60 cps), the filter output was considerably attenutated (fig. 7(c), left); at the third harmonic the attenuation was practically complete. The other record (fig. 7(c), right)

yields the absolute value of the filter output when the input is a signal produced by the simulator operating near its peak value under conditions of hysteresis.

RESULTS AND DISCUSSION

The particular control described by figure 6 was "set up" on an electronic differential analyzer for study and analysis. Various control variables were recorded during stable peak holding action, and measurements were made of peak average output and filter-output values at the point of "best stability." The effect on stability of such design parameters as band-pass center frequency, band width, and loop gain were determined; and general control action is discussed.

Typical Recordings of Control Action

Several analog solutions of the control are presented in figure 8. An arbitrary forcing bias $-C$, which could be some control function such as speed error in a gas-turbine engine, was integrated to supply a ramp velocity (fig. 8(a), trace 3). A perturbation was superimposed on the ramp (trace 5) which served as the input e_i to the simulator. The simulator output is shown as trace 4. When the output reached the maximum value E_3, wave trains appeared at the filter output $G(p)$ (trace 1). The filter was adjusted to minimum band width and a center frequency of the third harmonic. The amplified absolute value of the filter output appears as trace 2.

Control action can be described as follows: Figure 8(a) is a recording of important parameters when the control is operating at the best stability condition with moderate ramp velocity. Initially there is a ramp velocity determined by the forcing bias and integrating rate. The moment maximum output is reached, the action of the control starts to reduce the ramp velocity to zero. The main stability criterion is the vanishing of the integrand; that is, the forcing bias must be equal and opposite to the amplified average absolute value of the filter output.

If the gain of the absolute-value device is further amplified, a higher forcing bias must be used to maintain the best stability. This is illustrated in figure 8(b). The resulting ramp velocity is increased, and the maximum output value is reached in less time. However, the integrator output becomes more oscillatory.

The forcing bias need not be equal and opposite to $K|G(p)|$. When it is less than the average absolute value of the filter output (fig. 8(c)), the control behaves as though it is too sensitive to the sudden

drop at maximum output. The resulting filter output reduces the input to the simulator faster than the forcing bias increases it. For the particular conditions shown in this recording, the maximum output is sampled on alternate cycles only.

When the forcing bias is too large (fig. 8(d)), the control cannot arrest the input when maximum output is reached. The sampling of the sudden drop in the output reduces the ramp velocity, but it is not reduced to zero. Eventually, the input drives the output completely into the undesirable region of operation.

In figure 8(e), the sudden drop in the output E_1 has been reduced. The generated signal at the output of the absolute-value device also decreases. This result indicated a smaller value of forcing bias to maintain best stability. The ramp velocity is considerably decreased.

The effect of hysteresis is shown in figure 8(f). At the maximum output, the ramp velocity not only reduces to zero, but it is also made momentarily negative. The recovery from the sudden drop occurs at a latter part of the perturbation period and is equal to an output value less than maximum.

In the hysteresis cases, it is possible to obtain two stable peaks (fig. 8(g)). This condition is due to the existence of a double value in the rectified filter output. There are two points at which the areas per unit time under the rectified filter output are equal; one point exists for a short-pulse duration, the other for a longer-pulse duration.

The analog solutions presented in figure 8 were recorded with galvanometer elements. These elements were not critically damped and had dynamic behavior that caused overshooting following sudden drops in the simulator output. An oscilloscope used in recording two simultaneous functions during alternate periods (fig. 9) indicated that the dynamic error was due to the recording equipment.

The upper photograph on the left side of figure 9 includes alternate input and output values of the controlled simulator during peak stable operation for no hysteresis. The lower photograph is for a condition of hysteresis. The pressure drop and recovery from the drop are instantaneous. The duration in undesirable operation (pulse width) is less for the case of no hysteresis.

The upper photograph on the right side of figure 9 illustrates the relation between the controlled output of the simulator when it is near maximum and the output of the absolute-value device. The lower photograph is a record of the same functions when the controlled output is maintained at the second stable point. The pulse width covers nearly

the entire cycle during which the simulator is operating in the undesirable region. The ringing time of the filter for this case is less than the pulse duration; that is, the transient caused by the sudden output drop had time to completely attenuate before recovery was caused.

Measurements of Average Values at Best Stability

The average simulator output and average absolute-value-device output were measured at the peak values under conditions of best stability with appropriate averaging meters. These values were measured to determine the effect of control design parameters on stability. The parameters varied were band-pass center frequency, band width, magnitude of output drop at maximum output, width of inert zone in input, perturbation amplitude, and gain of absolute-value device.

The data for figures 10 to 12 were obtained when the control was acting in its most stable manner. This occurred when the forcing bias was approximately equal and opposite to the average output value of the absolute-value device. The effect of varying the band-pass center frequency and magnitude of drop at maximum output E_1 is shown in figure 10(a). The peak average output increases with band-pass center frequency but decreases with increasing output drop. The output of the absolute-value device decreases with increasing center frequency but increases with increasing output drop. The maximum usable forcing bias varies with the output of the absolute-value device. Thus, larger output drops permit a faster ramp velocity but cause the peak average output to reduce.

The effect of varying the filter pass band width is illustrated in figure 10(b). The peak average output decreases with increasing band width and with the size of the inert zone in the input. The output drop is kept constant. The average output of the absolute-value device increases with increasing band width and inert zone. This permits faster ramp velocities to be associated with the wider band widths.

Hysteresis effects are shown in figures 11(a) and (b). The peak average output decreases with increasing inert zone and with increasing output drop. The average output of the absolute-value device remains essentially constant with variation of inert zone but again increases with output drop.

As the perturbation amplitude increases, the peak average output decreases (fig. 12). However, the average output of the absolute-value device, and hence the ramp velocity for best stability, remains constant. The time delay and lag of the actual filter, coupled with the voltage drop across the diodes contained in the simulator (see fig. 17), did not permit the pulse duration to reach zero. Therefore, the perturbation amplitude must be at least equal to the inert-zone width for the control to operate properly.

[redacted]

The peak average output of the controlled simulator did not vary with the gain of the absolute-value device (fig. 13). The output of the absolute-value device varies linearly with its gain and allows the ramp velocity to vary accordingly.

Analysis of Control Behavior

The control is an example of a servo (including computor) operating with pulse data (ref. 2). The control begins operating with an initial error (forcing bias). Immediately after a drop occurs in the output, a measurement is made and the error is decreased. After the next measurement, the error is again decreased. Instability can result from either overcorrection or undercorrection. Initially, the forcing bias is acted upon by only the forward part of the loop. When the peak is approached, the discontinuities present in the simulator produce pulse inputs to the filter, and the loop is closed. Thus the control depends heavily upon the performance of filters with pulse input data.

The transfer function of the actual filter used is given in figure 7(a). If, for simplicity, the filter is assumed critically damped (i.e., $\sin \omega_0 t \approx \omega_0 t$), its indicial response would be as shown in figure 14 (ref. 3). This theoretical solution agrees with the measured solution recorded in figure 7(b) as do also the absolute values. The dominant feature of the response (absolute value) is an oscillation whose period is short compared with the important time constant of the control system, the integrating rate. The integral of the absolute value of the filter response is given in figure 15. For $\alpha t < 1$, the integral is approximately zero; for $\alpha t > 20$, the contribution to the integral is approximately zero. Thus the corrective value existing as feedback at the time αt can be approximated as dead time plus first-order lag. This corrective action exists only after a sudden drop in the output is experienced.

The continuous operation of the control loop can be used in studying stability during corrective action. Initially, the forcing bias provides a ramp input that drives the output toward its maximum value. Superimposed on the ramp input is the perturbation signal $A \sin \omega_0 t$. The instant the input reaches a value causing maximum output, the sudden drop in the output introduces a step into the filter. This step produces the response given by figure 14, whose integral (fig. 15) becomes the corrective value.

For pulses whose duration is short compared with the perturbation period, the shape of the absolute value of the filter response resembles that due to a step input. Therefore, for simplicity, a step input to the filter will be considered.

The ramp velocity (fig. 16) initially is

$$\frac{1}{\alpha\tau}\int^{\alpha t} C\, d(\alpha t)$$

and the input to the simulator at any time is the sum of this and the instantaneous value of the sinusoidal variation. When this input is at the maximum value, a step is introduced into the filter. The integral of the absolute value of the filter output is

$$\frac{K}{\alpha}\int^{\alpha t} |G(s)|\, d(\alpha t)$$

This integral acts to reduce the ramp velocity to zero (end of region 1). At this time, the integrals are equal but opposite. Because the corrective action exists only during part of the perturbation period, the ramp velocity must be made negative (region 2) to ensure that the input remains below the value corresponding to maximum output.

The corrective integral (fig. 15) tends to a maximum value; the ramp integral is constantly increasing. Therefore, the two integrals will again produce a zero ramp velocity (end of region 2). Thus, zero ramp velocity occurs twice during each perturbation period if the forcing bias is made equal and opposite to the average absolute value of the filter output. This is the condition for best stability.

If the corrective action is insufficient, the control is unstable in that it drives the output into the undesirable region (beyond peak output, fig. 8(d)). If the corrective action is too great, the control will cause operation below the peak output. Peak output will not be reached during every cycle of the perturbation period (fig. 8(c)). When the corrective action is exactly sufficient, the peak value will be reached every perturbation period (fig. 8(a)). Proper operation thus constitutes a sampling type of peak holding control.

SUMMARY OF RESULTS

A typical plant process was studied in which the output increases with input up to a certain maximum value, and further increases cause the output to drop suddenly into an undesirable region of operation (turbojet-engine operation in the vicinity of stalled compressor performance). The information was incorporated into a specially designed function generator that simulated the process.

The simulator was used to investigate the possibilities of a peak holding type of control. Sinusoidal variations in the input to the simulator resulted in a distorted variation in the output when the output was near its peak value. The generated information was used as negative feedback to maintain the peak value.

The control investigated maintained an average output less than that realizable when the input was at the maximum value. The average output was directly related to the perturbation amplitude, the magnitude of drop occurring at the peak, and the width of the inert zone in the input. It also depended on the center frequency and band width of the band-pass filter used to measure harmonic content. The ramp velocity depended on the feedback path gain and magnitude of drop at the peak value.

The control was stable for all ramp velocities below some optimal velocity that depended on both loop gain and magnitude of drop. At the optimal setting, the ramp velocity was maximum and the input had minimum variation.

Lewis Flight Propulsion Laboratory
National Advisory Committee for Aeronautics
Cleveland, Ohio, December 2, 1955

APPENDIX A

SYMBOLS

A	perturbation amplitude, v
a,b	Fourier coefficients
C	forcing bias, v
D_1,D_2,D_3,D_4	diodes
E	voltage
E_1	voltage simulation of Δp
E_2	voltage simulation of inert zone in input
E_3	voltage simulation of $\overline{\Delta P}$
e	corrective voltage, v
e_b	feedback voltage, v
e_i	instantaneous input voltage, v
e_o	instantaneous output voltage, v
f,G	functional relations
K	feedback path gain
$\frac{K}{2}\overline{\lvert G(s)\rvert}$	average absolute value of filter output, v
$\mathcal{L}^{-1}$	inverse Laplace transform
m	slope, $\Delta P/\Delta w_f$
N	engine speed, rpm or percent rated
$\dot{N}$	acceleration, rpm/sec
n	Fourier series harmonics
ΔP	pressure change from equilibrium, lb/sq in.
$\overline{\Delta P}$	maximum pressure increase, lb/sq in.

$\overline{\overline{\Delta P}}$	average output pressure, lb/sq in.
Δp	pressure drop at maximum, lb/sq in.
s	Laplace operator
T	perturbation period, sec
t	time, sec
w_f	fuel flow, lb/hr
Δw_f	fuel-flow change from equilibrium, lb/hr or percent rated
$\overline{w}_f$	input fuel-flow level
$\overline{\Delta w}_f$	fuel flow corresponding to $\overline{\Delta P}$
α	filter parameter, radians/sec
μ	amplifier gain
τ	integrator time constant
τ_c	$\omega_c/2\pi$, sec
τ_1,τ_2	band-pass-filter variables
φ	$\omega_0 t$, radians or deg
φ_1	stall inception angle, radians or deg
φ_2	stall recovery angle, radians or deg
ω_c	band-pass-filter center frequency, radians/sec
ω_0	perturbation frequency, radians/sec

APPENDIX B

COMPRESSOR SIMULATION

A typical engine was studied for its pressure response to fuel-flow changes with particular emphasis on its stall behavior. The sharp pressure drop at stall (fig. 1(a)), the associated dead zone during stall, and the hysteresis loop that the combination implies was duplicated by an amplifier-diode circuit. A comparator coupled to a series output limiter was connected in a closed loop to form a modified bistable multivibrator, and the response of the multivibrator was summed with another series output limiter. The result was a function generator that approximated, in a simplified manner, the dynamic behavior of the compressor.

The comparator reference voltage duplicates the stall point, and the limiter determines the size of the dead zone. The comparator also determines the amount of the pressure drop. These nonlinear characteristics were reproduced by amplifier-diode circuits. The circuits used diodes having a high back impedance to produce abrupt changes in slope that depend on the magnitude of one or more voltages. Diodes rather than relays were used because they are faster and usually require less equipment. Diodes also permit the use of stabilized direct-current computing amplifiers. The error introduced by diode use is given in figure 17.

The analyzer circuit that simulates the instantaneous pressure drop at stall is the comparator (fig. 18(a)). A variable voltage E_1, which is a measure of the pressure drop at stall, figure 1, can be turned on or off at a coincidence of two other variable voltages, E_3 representing the pressure increase at stall and e_i representing the input fuel flow.

The comparator is a switch that operates when the input voltage e_i equals the negative of the reference voltage $(e_b - E_3)$. If $e_i = 0$, increasing positively, diode D_2 conducts and clamps the output to zero (within the error specified in fig. 17). When $e_i = E_3 - e_b$, a transition is initiated and D_2 stops conducting. Then, for a further incremental increase $\Delta e_i = E$, the full amplifier gain produces an output $e_o = -\mu E$. The output increases negatively until $-\mu E = -E_1$. At this value D_1 conducts and clamps the output to $-E_1$. Further increases in the input produce no further change in the output.

If $e_i = 0$, increasing negatively, D_2 conducts and clamps the output to zero. Thus the comparator has zero gain in either of its two stable states. The output must be either zero or $-E_1$ according to whether the sum of the input and reference is negative or positive. During the transition, the output slope is μ (70,000 for the amplifiers used).

In order to simulate dead zone (inert zone in fuel flow), a series output limiter is coupled to the comparator output and the limiter output is fed back to the comparator input to form a closed loop (fig. 18). The inert zone in fuel flow (approximated from such data as fig. 1) is then determined by E_2.

A series output limiter is defined as an amplifier-diode circuit employing one or more diodes in the feedback path that decrease the current through the summing node by diode conduction. It produces normal scale changing until some limiting value of the output is reached. For the given circuit (fig. 18(b)), the output slope is negative. If the input is positive, decreasing, the output is negative. As the input passes through zero, increasing negatively, the output passes through zero, increasing positively. When the input reaches a value for which the output is E_2, D_3 conducts and thereby clamps the output to E_2 for increasingly negative inputs.

The coupling of the series output limiter and comparator to form a closed loop (fig. 18(c)) forms a modified version of the well-known bistable multivibrator. In this circuit there is a hysteresis loop whose position and area can be independently adjusted; that is, the stall pressure E_3, the pressure drop E_1, and the inert zone E_2 can be independently adjusted to the values determined from engine data.

If the input voltage is initially negative, increasing positively, and the feedback voltage e_b is momentarily zero, D_2 conducts to clamp the output to zero. The output remains zero until the input is equal and opposite to $-E_3$ ($e_i - E_3 = 0$). At this value the transition to the other stable state starts. Then D_2 stops conducting. The output varies scalarly, with slope $-\mu$, with the input until it reaches the value $-E_1$.

The series output limiter provides positive feedback e_b to the comparator. During the transition the comparator output is limited to the value E_2. The feedback voltage does not disturb the comparator because it is positive and thus does not cause the value at the summing junction of the comparator to go through zero. Therefore, the output of the comparator remains at $-E_1$ for further increases in the input.

As the input reverses direction (becoming less positive), the output remains clamped to $-E_1$ until $e_i + e_b - E_3 = 0$. The comparator thus switches at the lower value $E_3 - e_b$ to zero output. The output remains clamped at zero for all values less than $E_3 - e_b$. After the transition, the feedback voltage again is zero, thus allowing the comparator to switch, in increasingly positive inputs, at the original value E_3. Note that for all $|E_1| < |E_2|$ the hysteresis loop remains square because the feedback voltage will not be limited by D_3 for this case.

In order to simulate pressure response to fuel-flow changes, a slope (fig. 19(a)) must be added to the multivibrator. As shown in the figure, the output slope is positive. If the input to the series output limiter is negative, the output is negative, and both will be zero at the same time. For an input increasingly positive, the output will also increase positively until it reaches a value E_3. At this value D_4 conducts and clamps the output at E_3 for further increases in the input.

When the outputs of the limiter and comparator are summed, a function generator is formed that simulates compressor dynamic behavior. If the comparator switches at E_3 and the limiter also limits at E_3, then for any set values of E_1, E_2, and E_3 an independent variable serving as a simultaneous input to both the comparator and limiter results in an output function as shown in figure 19(a). Specifically, if the input is fuel flow (100 v = 10,000 lb/hr), the output is the negative of the compressor-discharge pressure (100 v = 10 lb/sq in.). The slope at 0.01 (lb/sq in.)/(lb/hr) would be the pressure fuel-flow gain at constant speed (fig. 4).

The theoretical function-generator performance is shown graphically in figure 19(b). The proposed function generator was set up on a differential analyzer, and the actual output of the simulator is shown in figure 3. The voltage drops across the diodes, as shown in figure 17, are in evidence. Under the worst conditions the departure from the ideal response is on the order of 1 volt. When referred to a machine unit of 100 volts, this represents an error of 1 percent.

[redacted]

APPENDIX C

INSTRUMENTATION

Three separate recorders were used for solution recording:

(1) A continuously recording oscillograph to record time histories

(2) An oscilloscope to record instantaneous functions at two successive periods

(3) A function plotter to record the steady-state relation between an input and output function

Oscillograph

A standard oscillograph with galvanometer elements and light-sensitive paper was used to record time histories. The computing amplifier rating of 5 milliamperes and range of 100 volts dictated a minimum load impedance of 20,000 ohms. Galvanometer elements with a damped sensitivity of 2 inches per milliampere were used to provide a gradient of 40 volts per inch on the paper.

Oscilloscope

A standard, 5-inch, single-beam oscilloscope was used with a blue fluorescent tube having minimum phosphorescence. In conjunction with a Polaroid camera, transients were recorded that had a duration of one period of the disturbance function. Two successive periods were displayed on the single-beam cathode-ray tube by using an electronic switch and adder.

A sweep generator (fig. 20) operating at the test frequency of the control triggered a flip-flop circuit. The Eccles-Jordan trigger circuit driven from the sweep generator had cathode-follower outputs and produced a 30-cps square wave, that is, half the basic repetition rate.

Two particular solutions, occurring at successive periods (figs. 7 and 9), were displayed on the scope by the arrangement shown. The signal input from the switch turned on each of a pair of diodes on alternate cycles. Each of the two inputs was connected to a diode through a unit-gain (variable) amplifier. A signal from the other side of the switch was added to the two diode outputs. An adjustable resistor (separator) caused the displays from the two input signals to separate vertically on the cathode-ray tube. The signal path through the switch was

direct-coupled, thus the signals were switched provided the separating resistor was adjusted for zero separation. However, there was some noticeable switching transient.

Function Plotter

The function plotter was commercial equipment that had a writing speed of 12 inches per second on both axes. This plotter produced such figures as figure 4.

REFERENCES

1. Guillemin, Ernst A.: Communication Networks. Vol II. Ch. XI - The Transient Behavior of Filters. John Wiley & Sons, Inc., 1951.

2. James, Hubert M., Nichols, Nathaniel B., and Phillips, Ralph S, eds.: Theory of Servomechanisms. Ch. V - Filters and Servo Systems with Pulsed Data. McGraw-Hill Book Co., Inc., 1947.

3. Gardner, Murray F., and Barnes, John L.: Transients in Linear Systems. Vol. I. John Wiley & Sons, Inc., 1942.

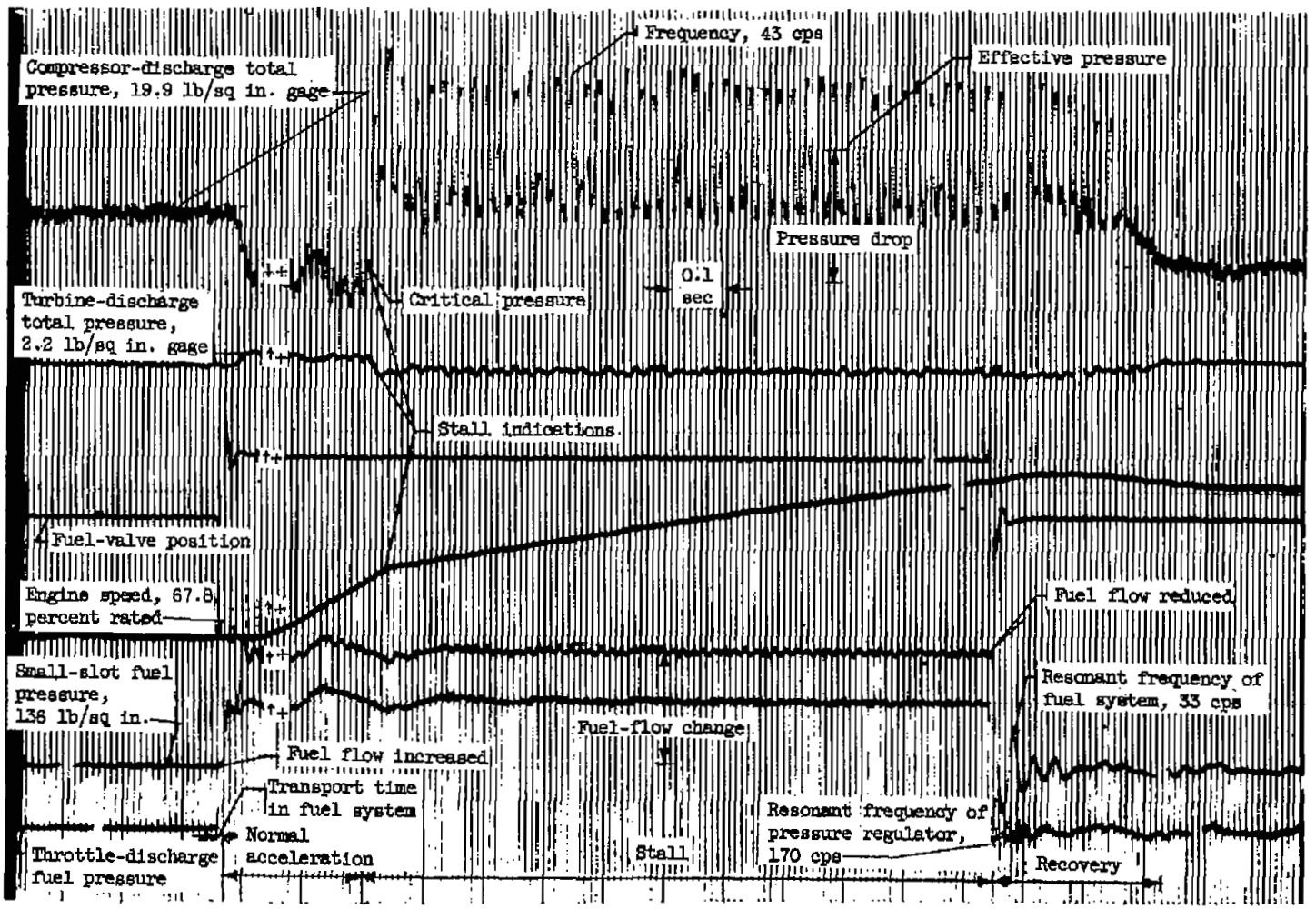

(a) Response of turbojet engine to sudden increase in fuel flow. (Calibration: compressor-discharge pressure, 6.96(lb/sq in.)/in.; turbine-discharge pressure, 8.3(lb/sq in.)/in.; engine speed, 200 rpm/in.; small-slot fuel pressure, 171(lb/sq in.)/in.)

Figure 1. - Typical turbojet-engine performance.

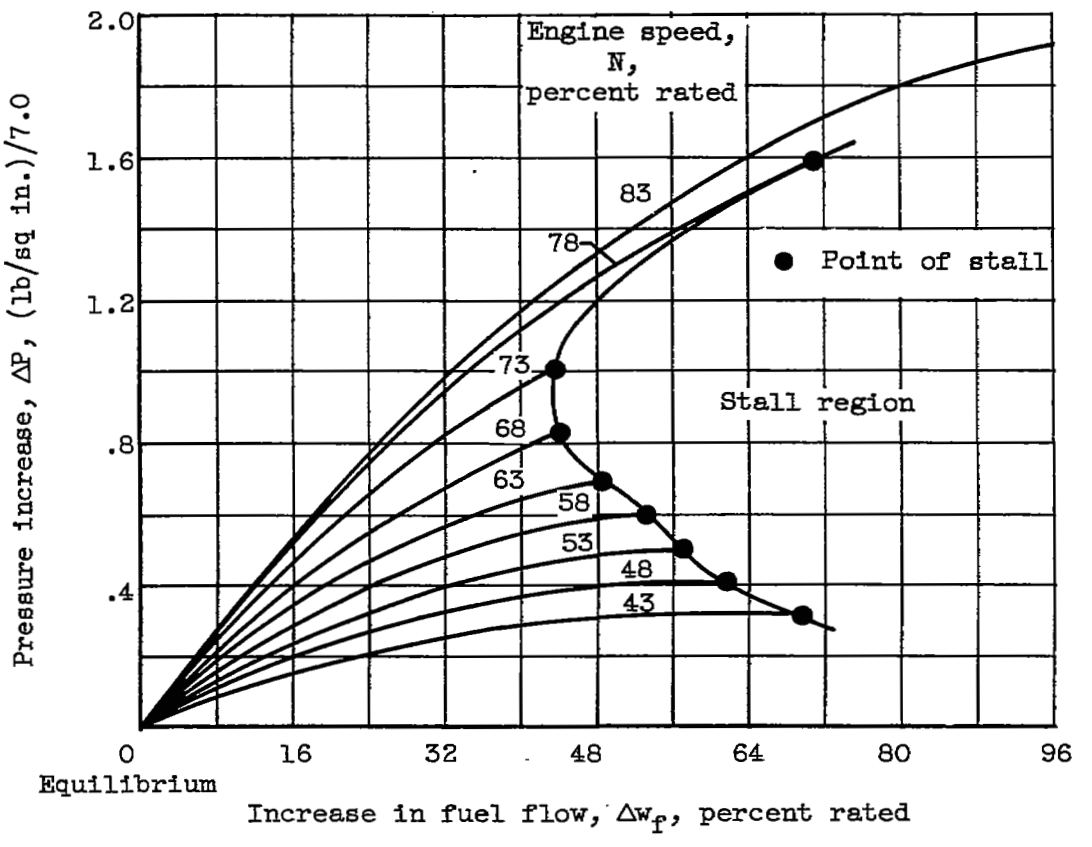

(b) Pressure change due to fuel-flow change at constant speed in vicinity of stall.

Figure 1. - Continued. Typical turbojet-engine performance.

[redacted]

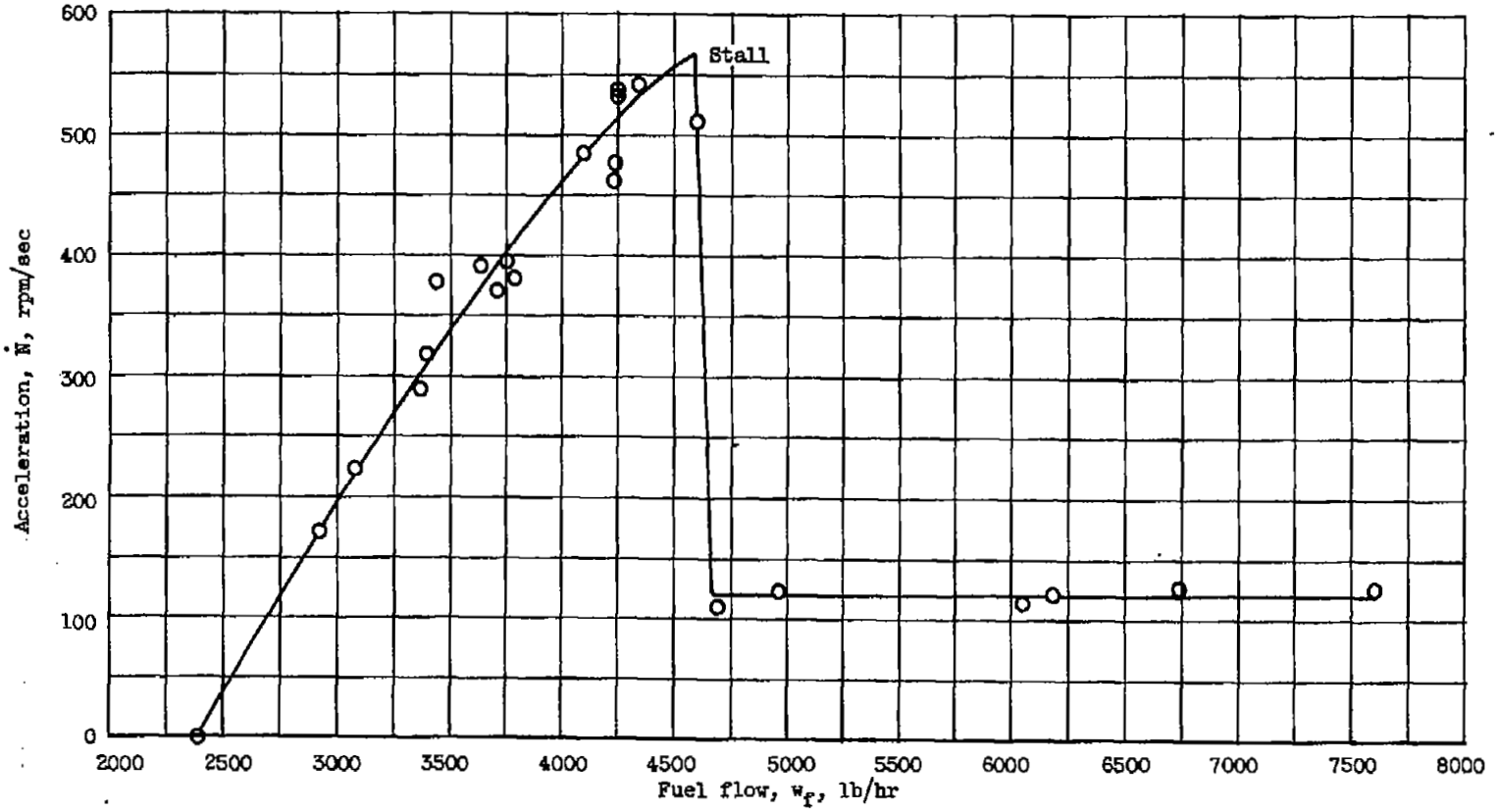

(c) Variation of acceleration with fuel flow. Engine speed, 70 percent rated.

Figure 1. - Continued. Typical turbojet-engine performance.

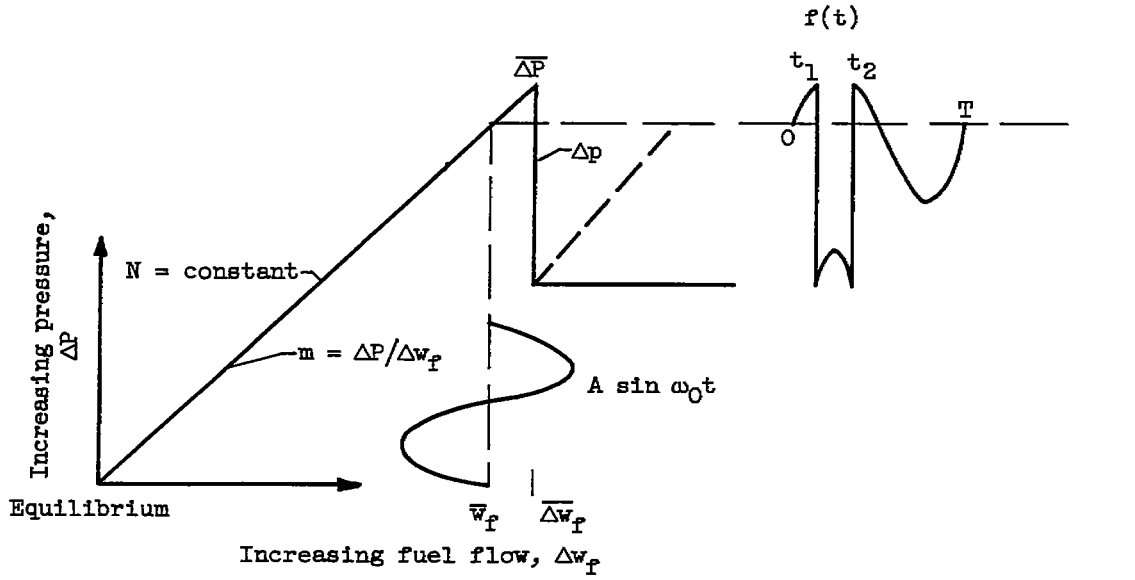

No hysteresis

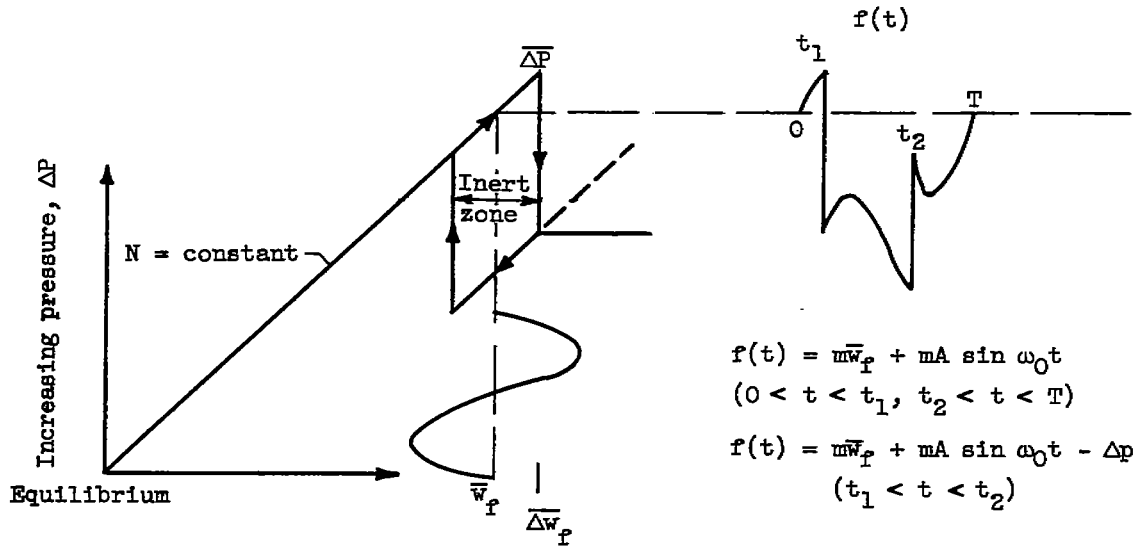

Hysteresis

(d) Idealized compressor response to forcing fuel flow. Constant engine speed.

Figure 1. - Concluded. Typical turbojet-engine performance.

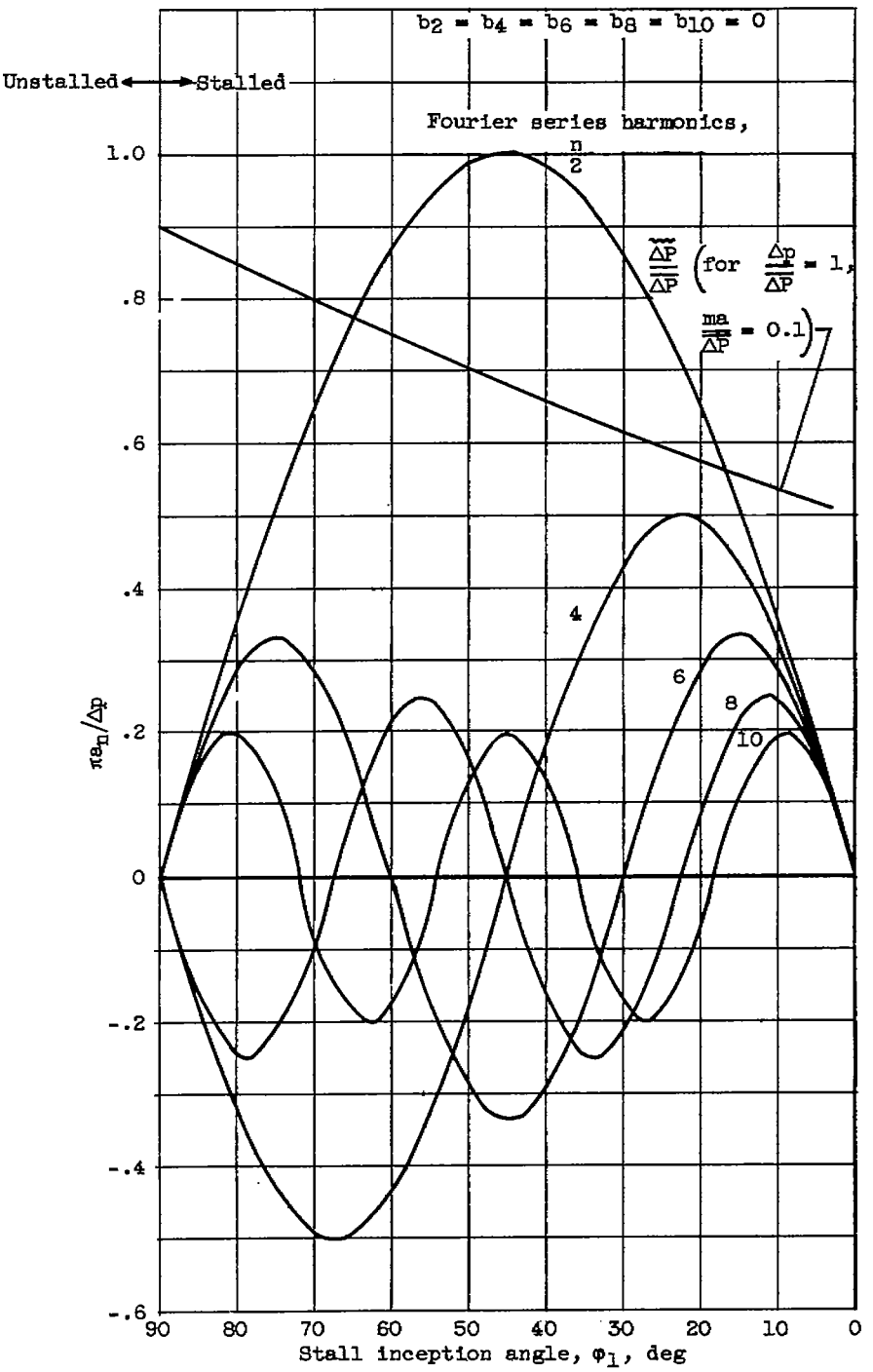

(a) Even harmonics.

Figure 2. - Harmonic content of function f(t) with no hysteresis.

[redacted]

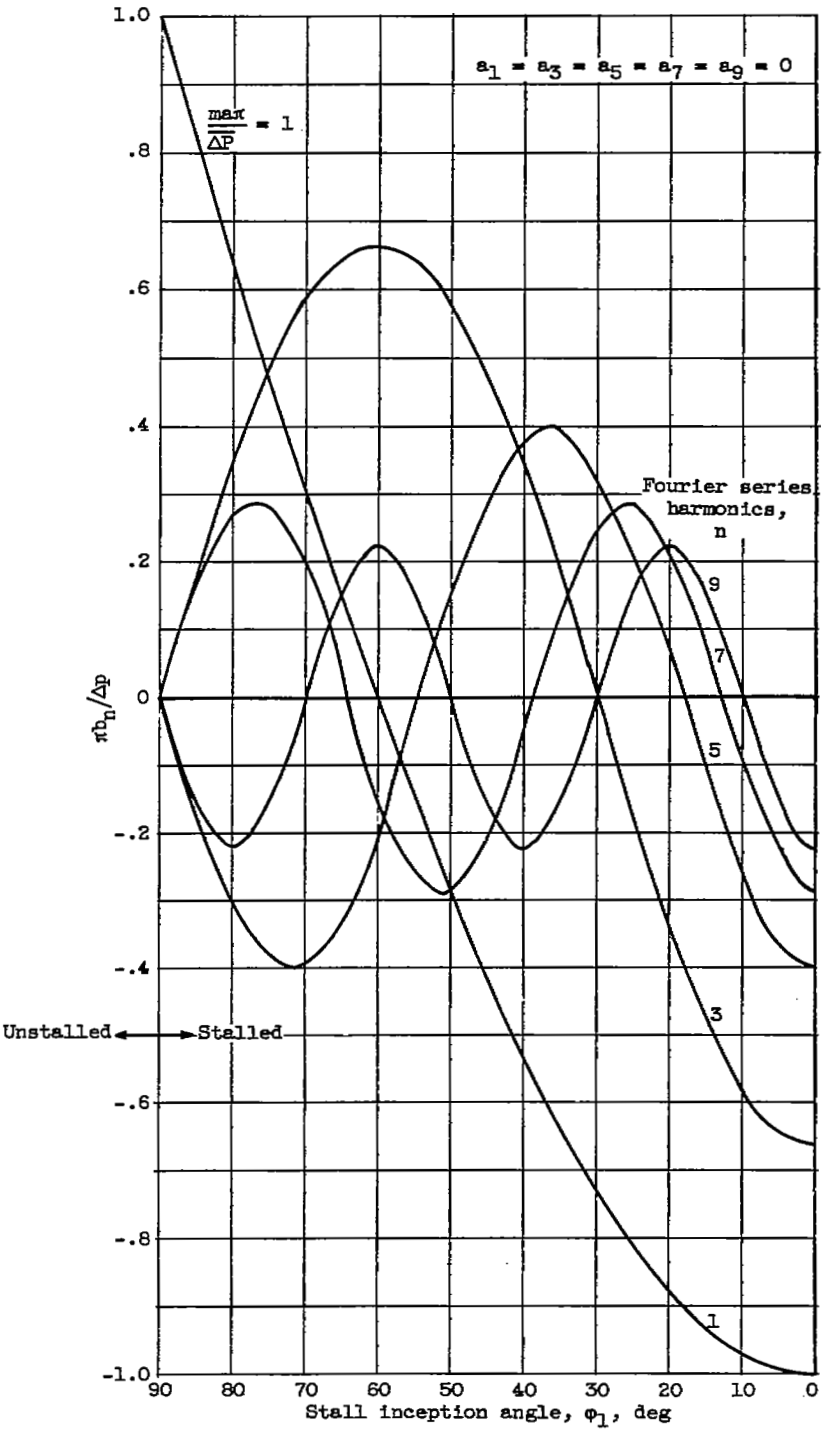

(b) Odd harmonics.

Figure 2. - Continued. Harmonic content of function f(t) with no hysteresis.

[redacted]

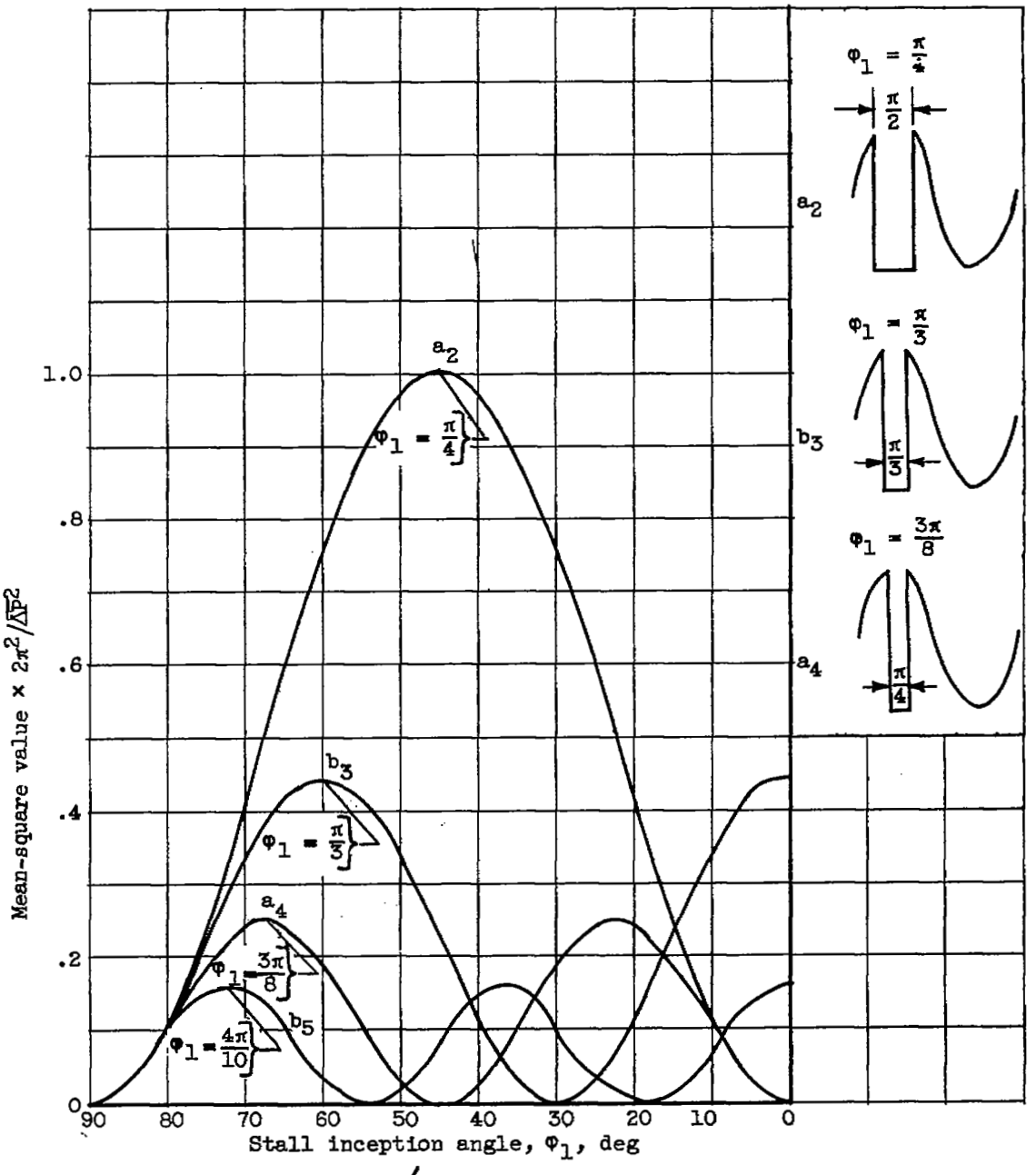

(c) Mean-square value. (Stall duration is π/n for maximum a_n or b_n, at zero ramp velocity, and stall inception is at $\pi/2\left(1 - \frac{1}{n}\right)$.)

Figure 2. - Continued. Harmonic content of function f(t) with no hysteresis.

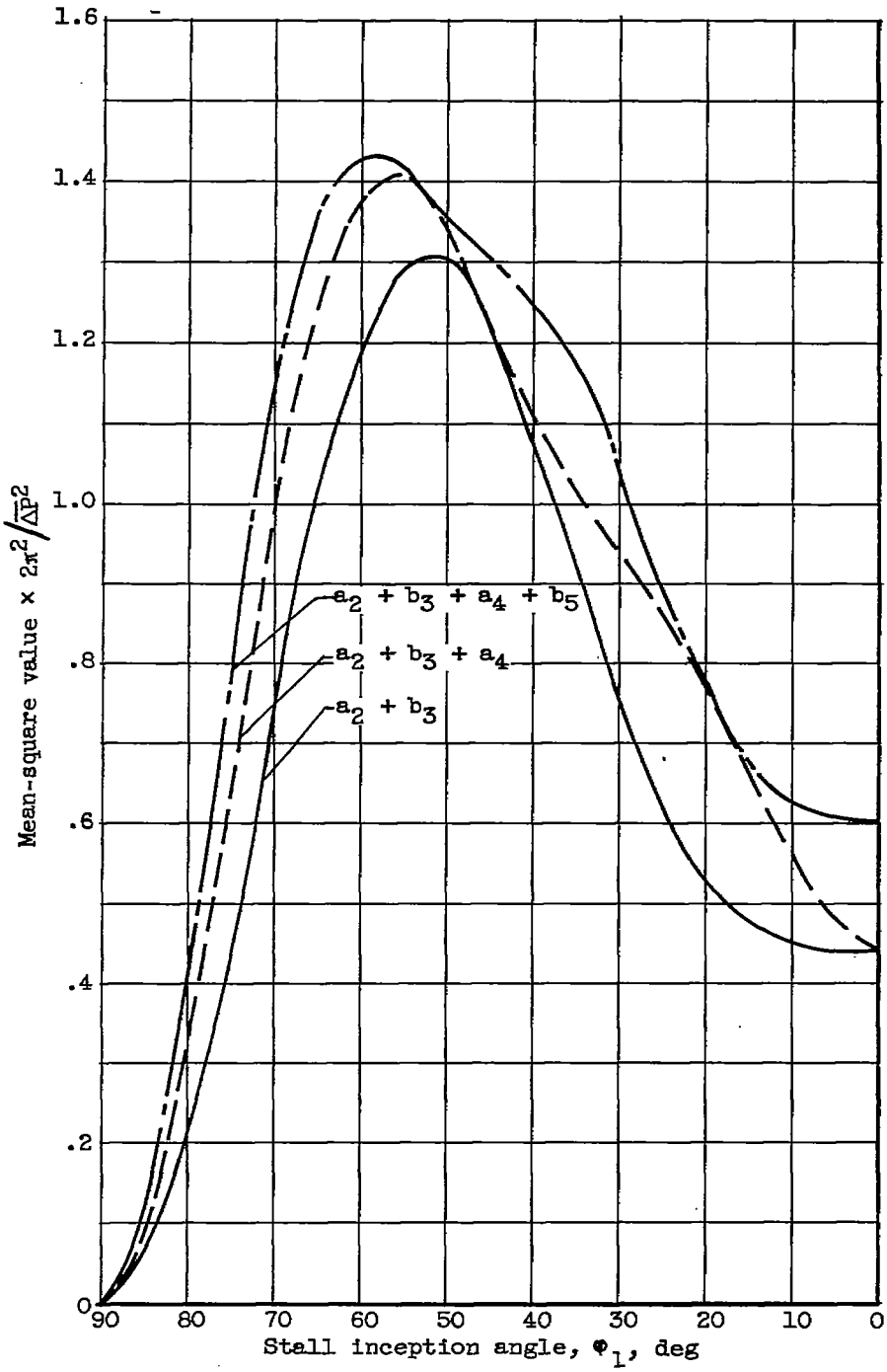

(d) Effect of summing the harmonics.

Figure 2. - Concluded. Harmonic content of function f(t) with no hysteresis.

[redacted]

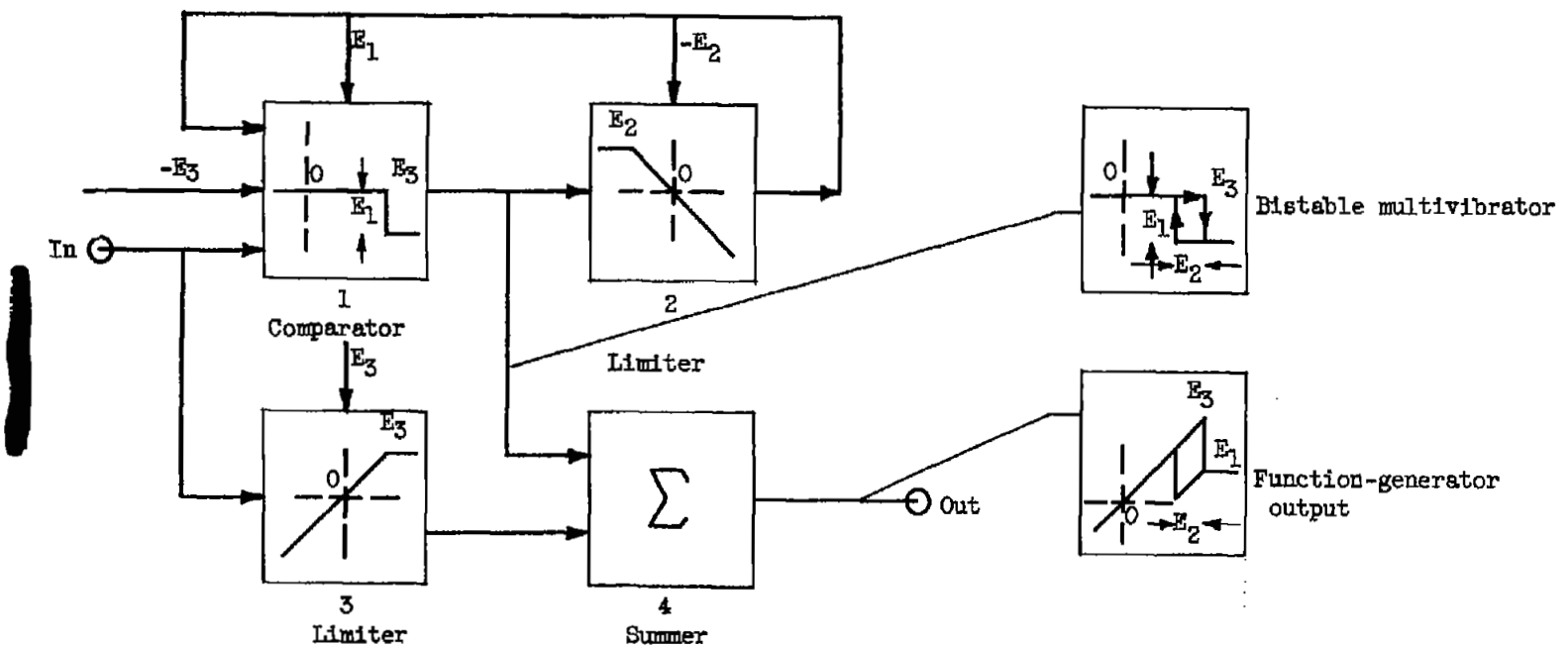

Figure 3. - Block diagram of simulator.

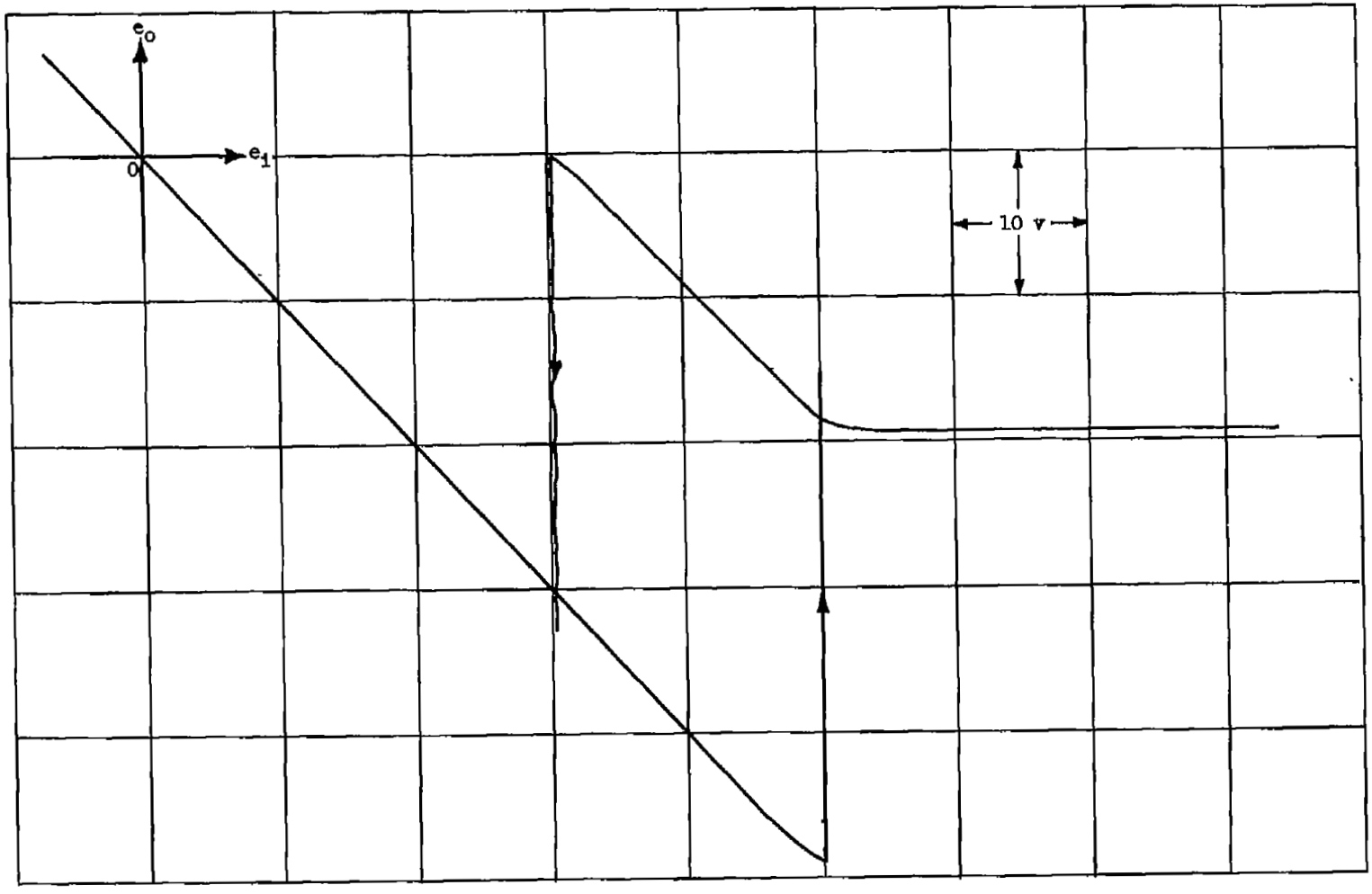

Figure 4. - Actual output of simulator. E_3 = 50.0 v; E_2 = 20.0 v; E_1 = 30.0 v.

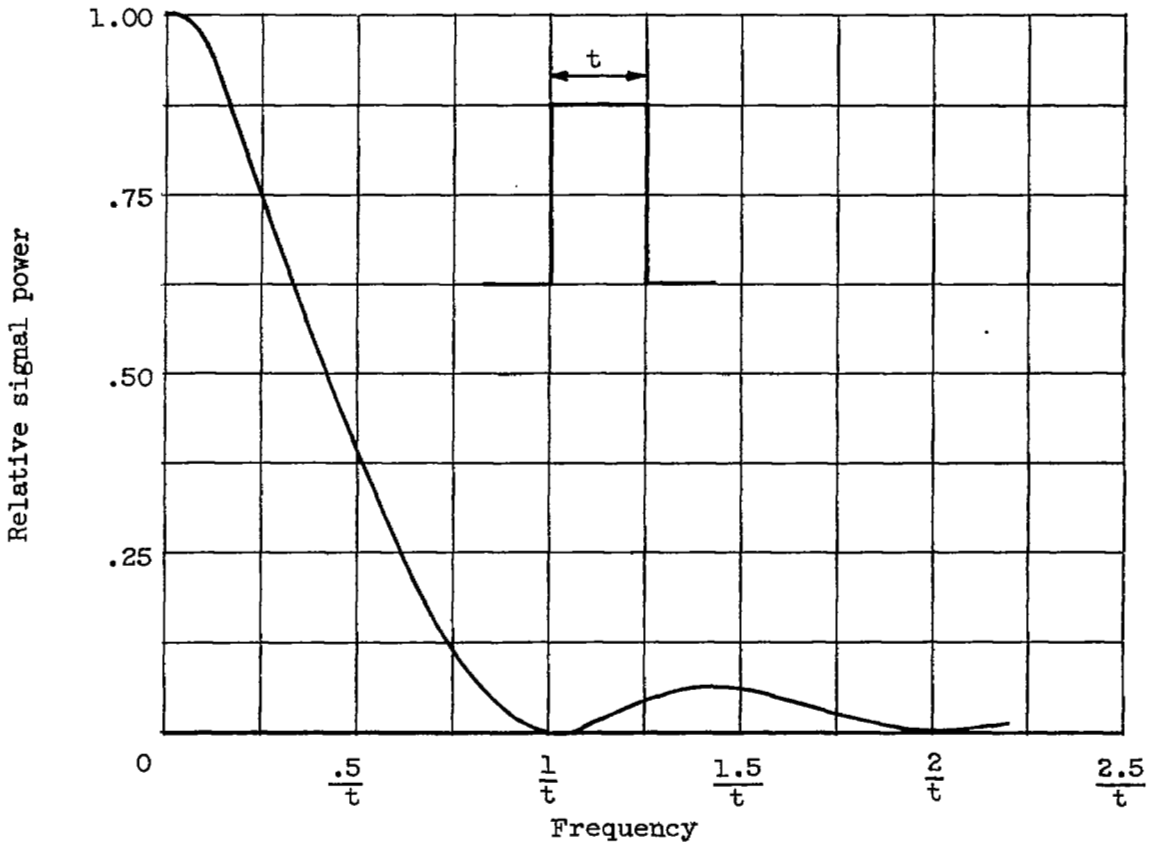

Figure 5. - Frequency spectrum of pulse.

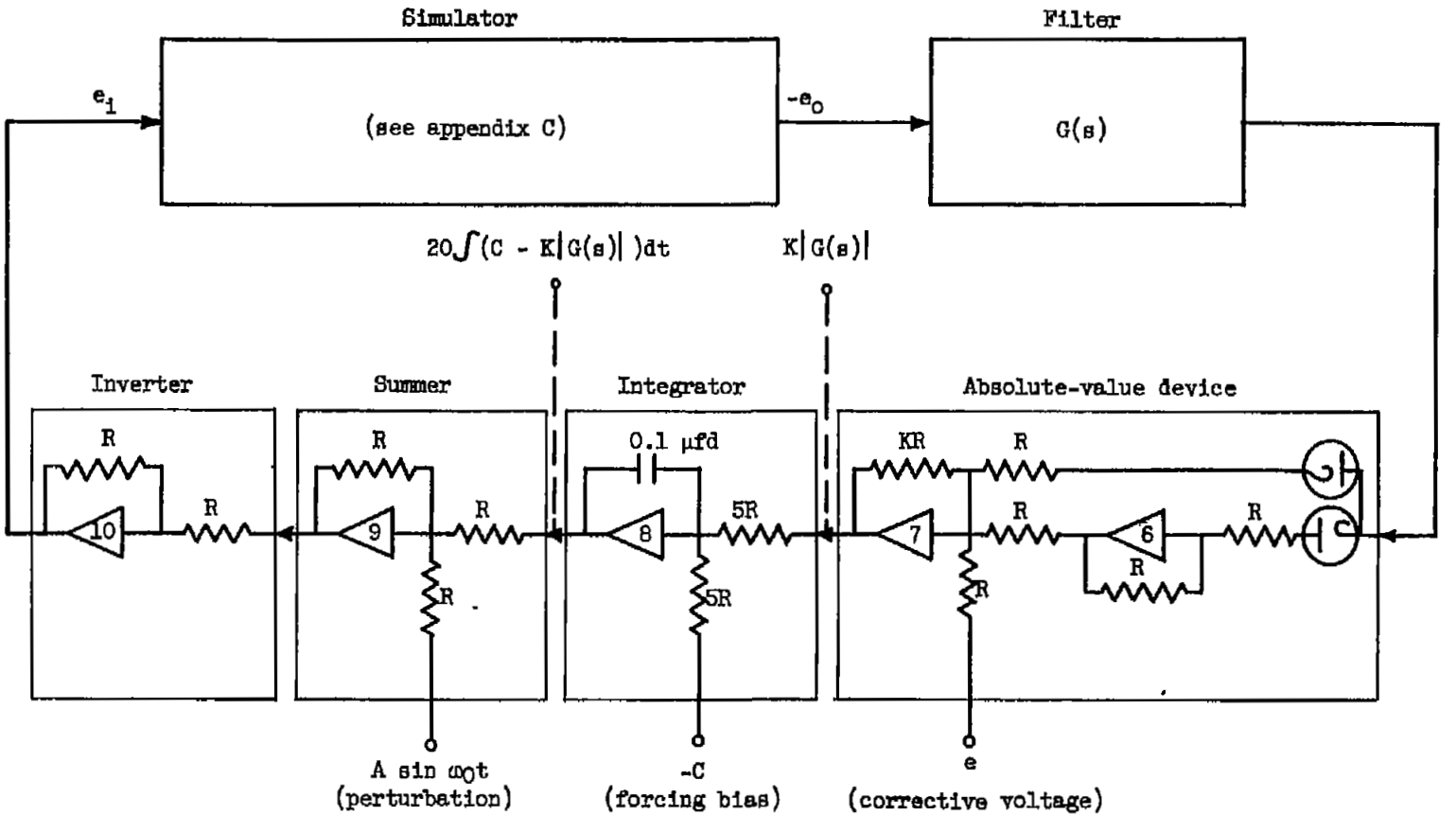

$$e_i = 20\int(K|G(p)| - C)dt - A \sin \omega_0 t$$

(a) Problem board wiring.

Figure 6. - Peak-holding-control loop.

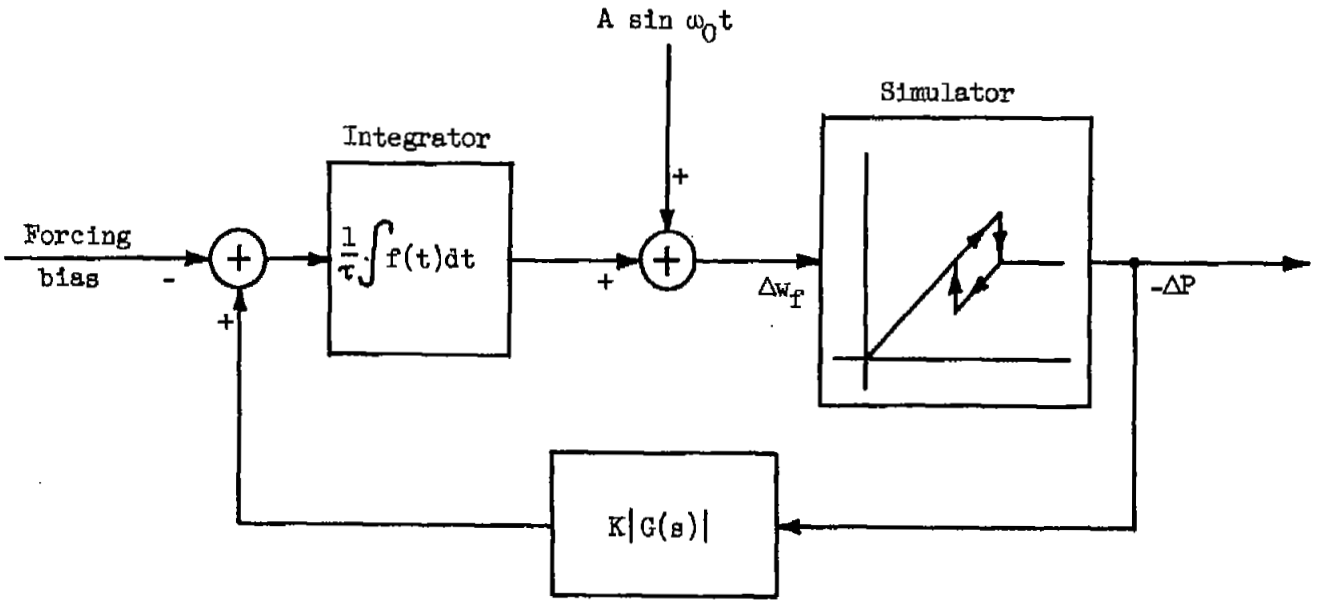

(b) Simplified block diagram.

Figure 6. - Concluded. Peak-holding-control loop.

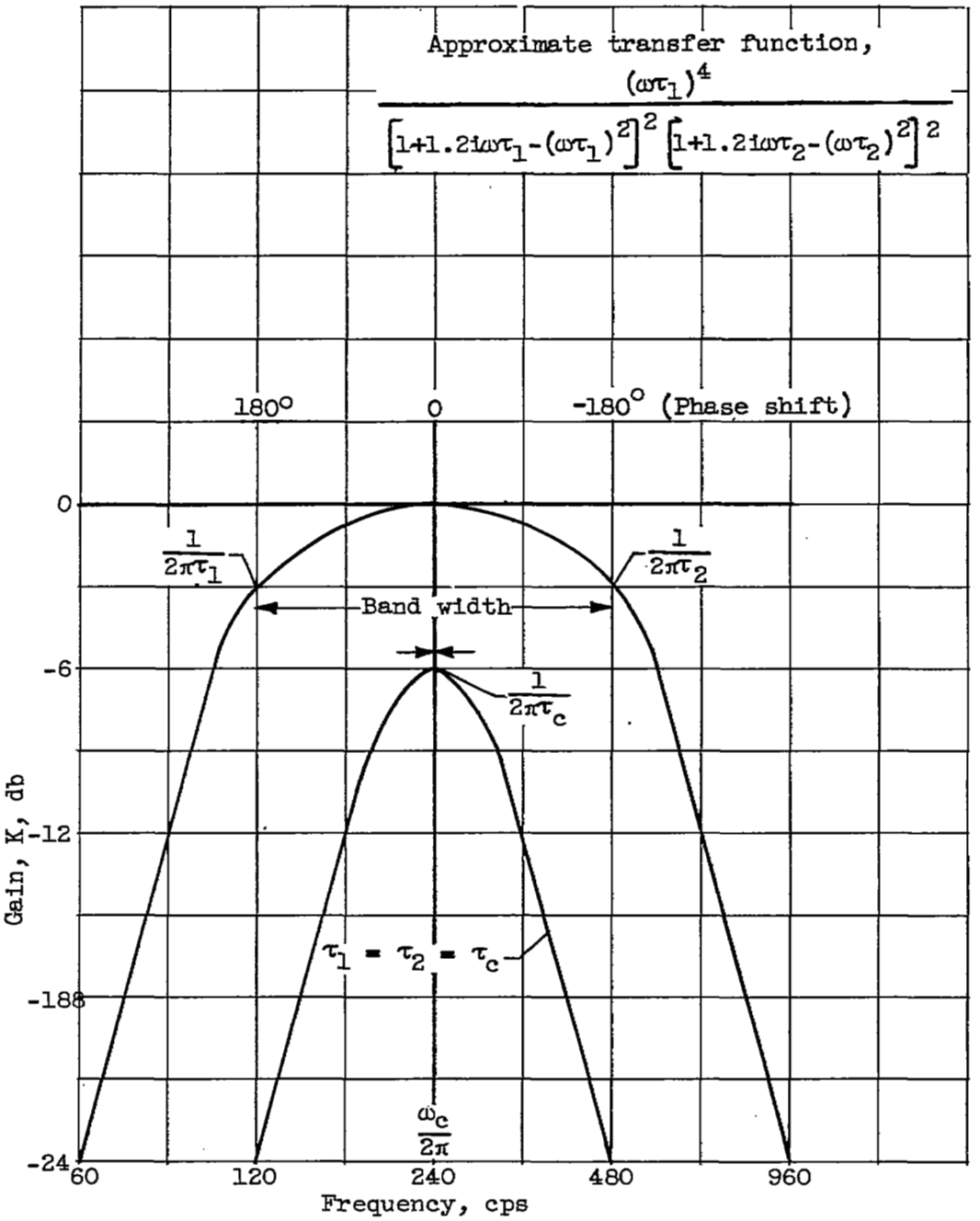

(a) Filter frequency response.

Figure 7. - Band-pass filter characteristics.

[redacted]

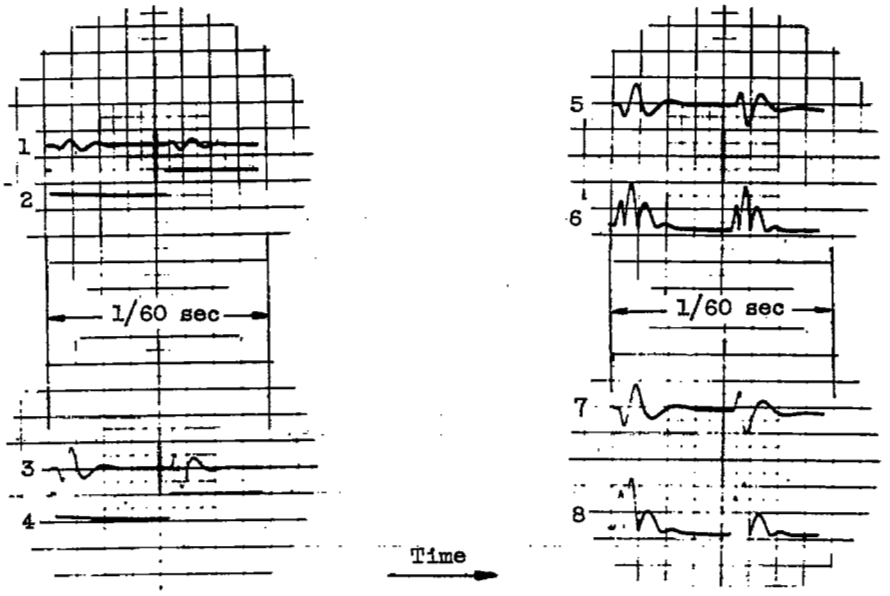

(1) Filter output (600-600 cps)
(2) Filter input
(3) Filter output (400-400 cps)
(4) Filter input

(5) Filter output (371-971 cps)
(6) Absolute value of (5)
(7) Filter output (315-1150 cps)
(8) Absolute value of (7)

(b) Filter responses to input pulses.

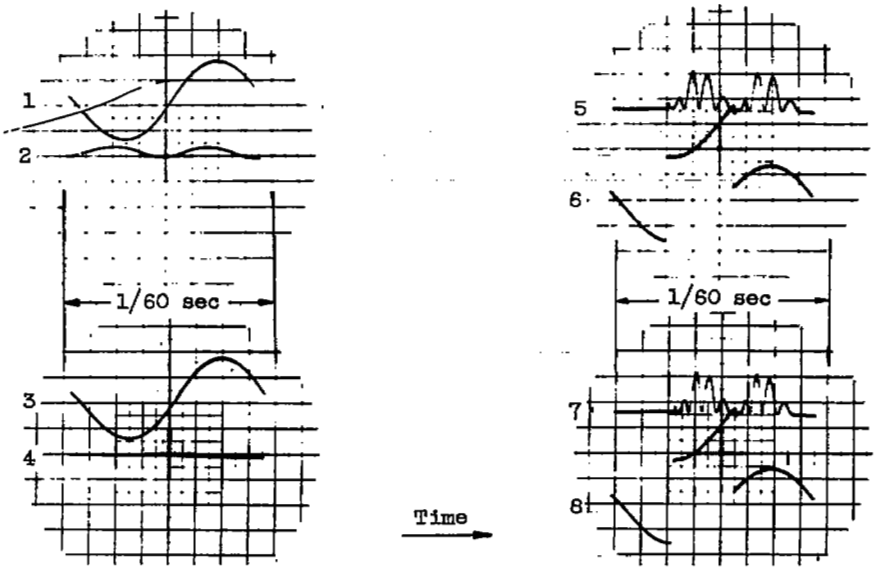

(1) Filter input (120-120 cps)
(2) Filter output
(3) Filter input (180-180 cps)
(4) Filter output

(5) Absolute value of filter output
(6) Filter input for (5) (420-420 cps)
(7) Absolute value of filter output
(8) Filter input for (7) (560-560 cps)

(c) Cut-off characteristics of filter, left; filter responses at peak conditions, with hysteresis, right.

Figure 7. - Concluded. Band-pass filter characteristics.

[redacted]

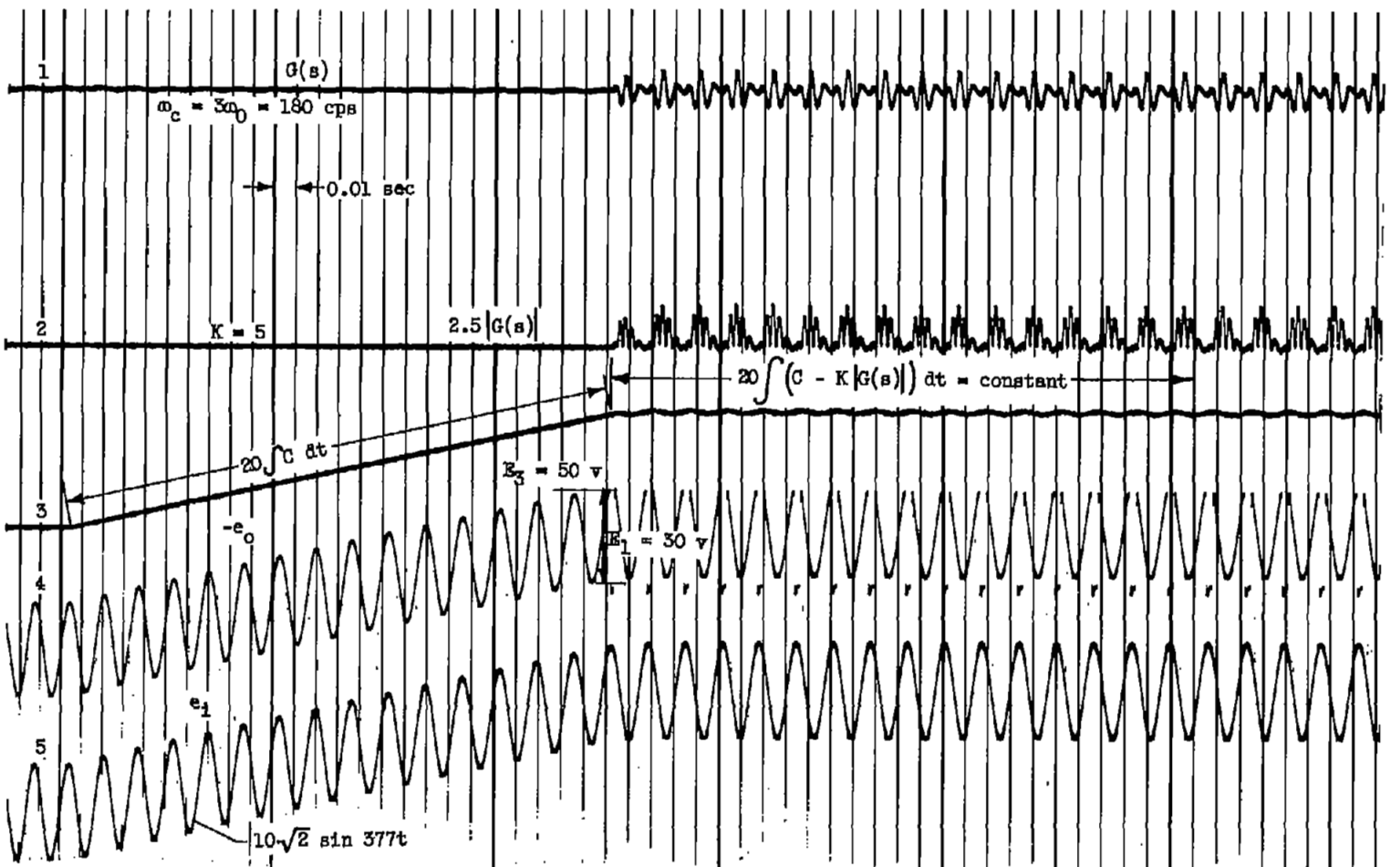

(a) Optimum stability condition and moderate ramp velocity. E_2, 0.

Figure 8. - Analog solutions of peak holding control.

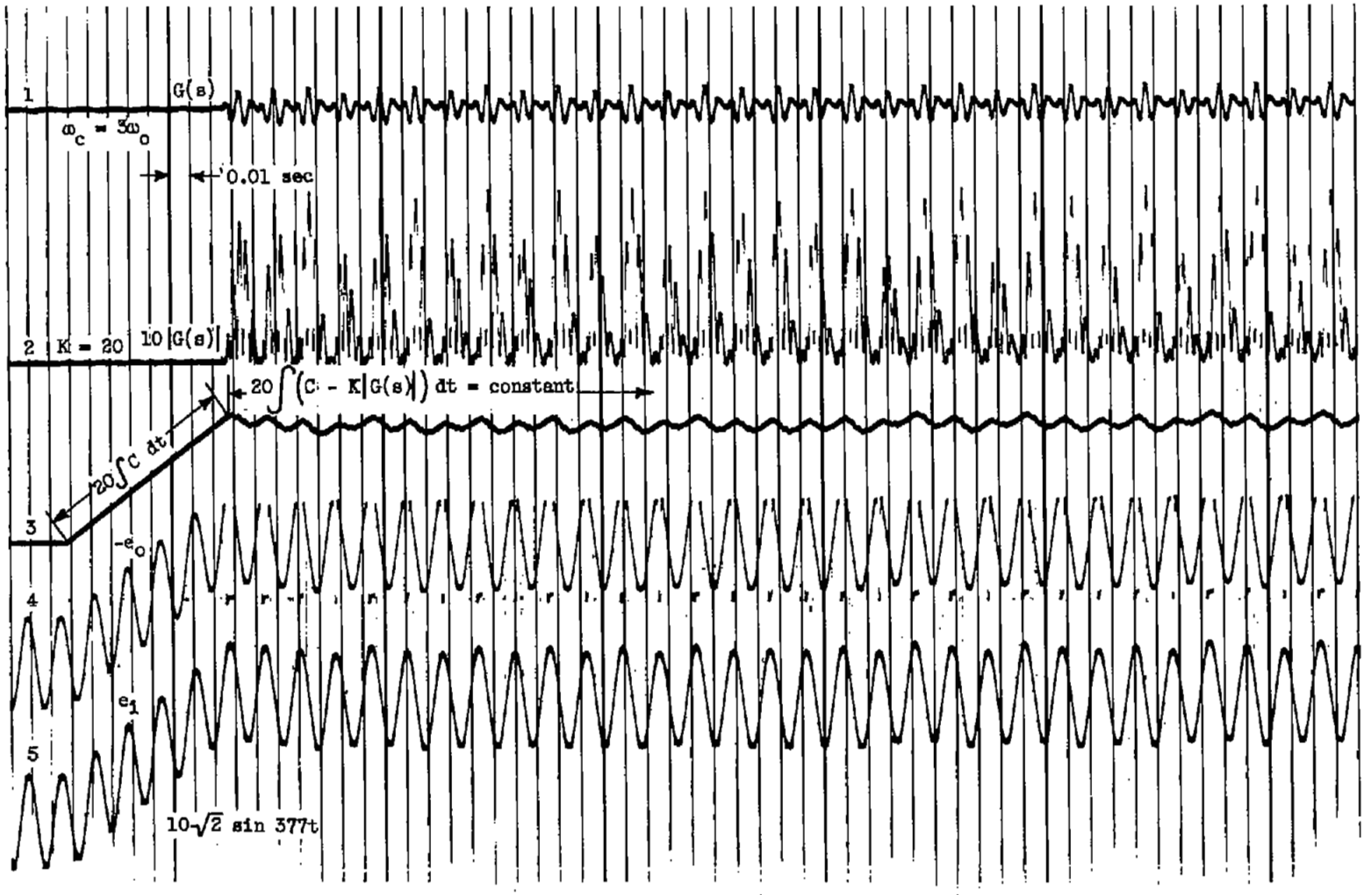

(b) Effect on stability of increased ramp velocity. E_1, 30 v; E_2, 0; E_3, 50 v.

Figure 8. - Continued. Analog solutions of peak holding control.

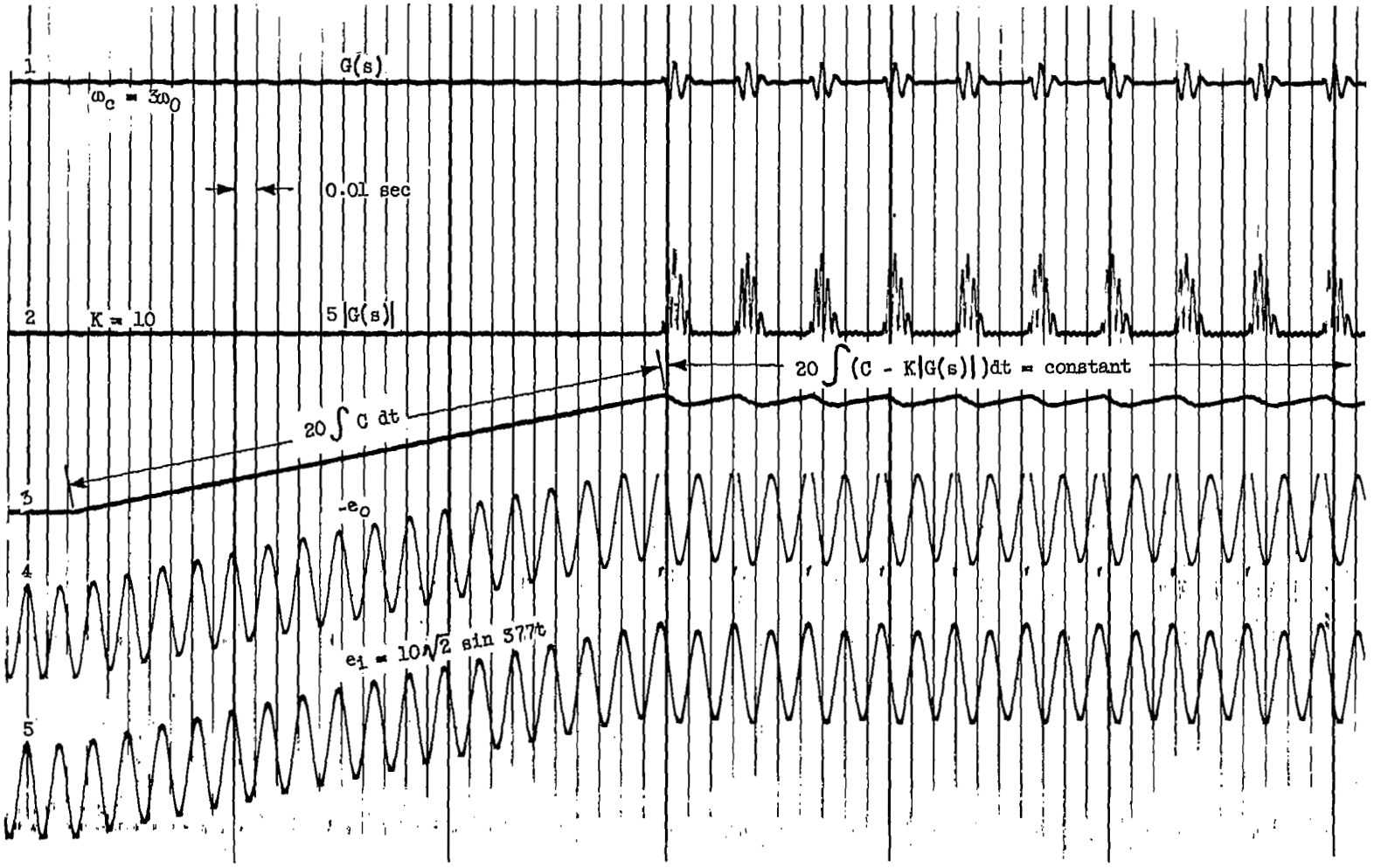

(c) Effect on stability of too low a forcing bias. E_1, 30 v; E_2, 0; E_3, 50 v.

Figure 8. - Continued. Analog solutions of peak holding control.

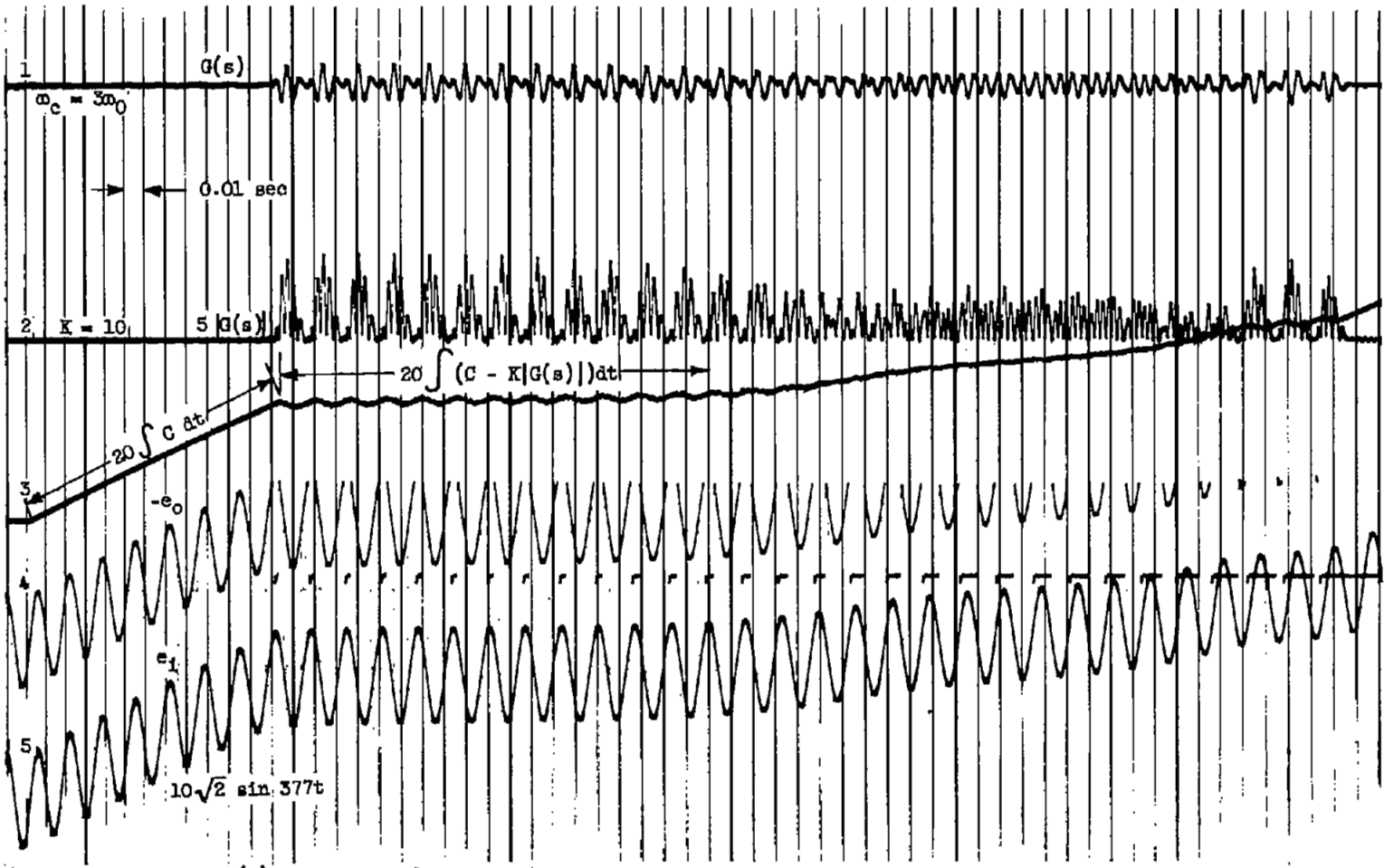

(d) Instability due to too large a forcing bias. E_1, 30 v; E_2, 0; E_3, 50 v.

Figure 8. - Continued. Analog solutions of peak holding control.

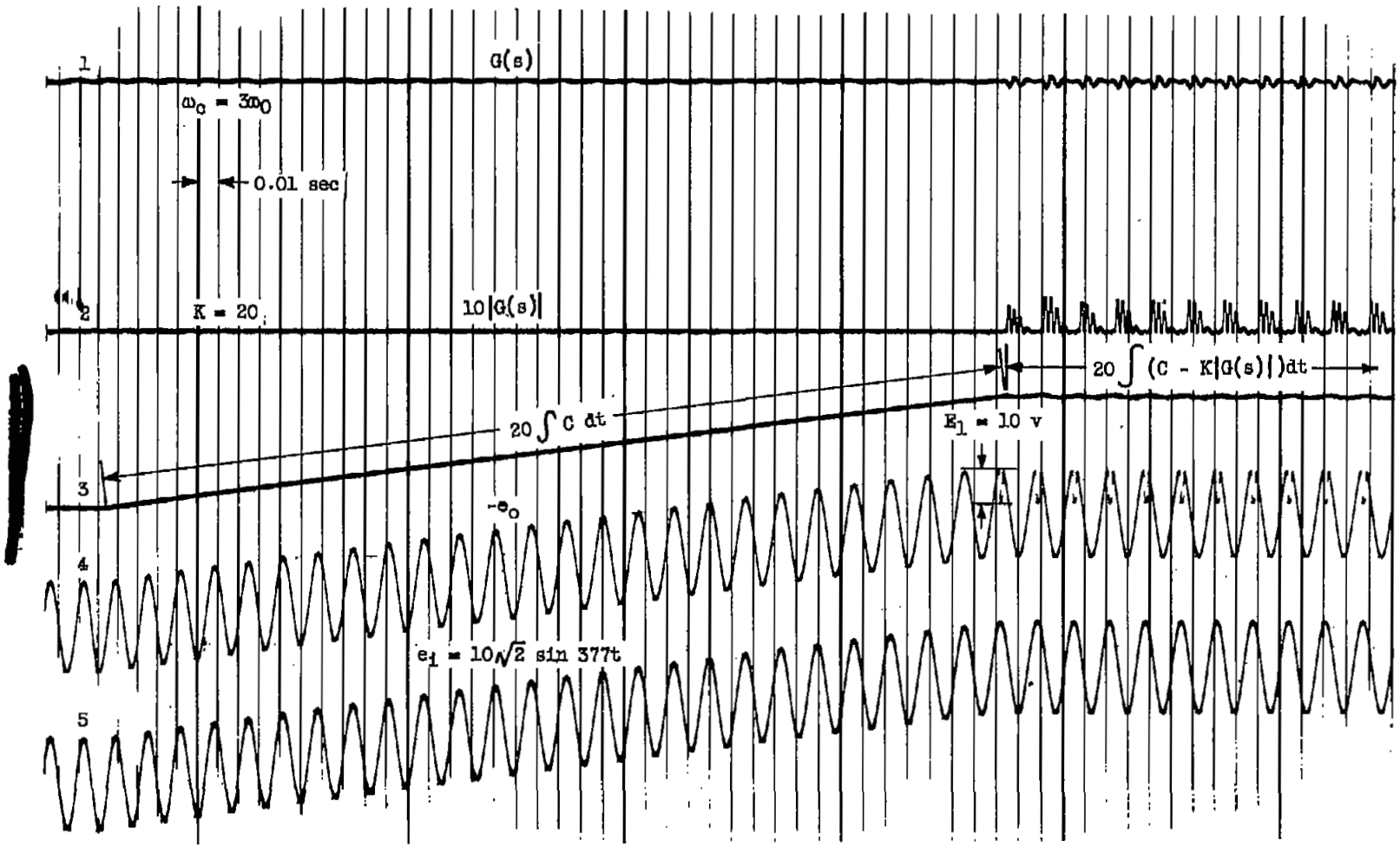

(e) Effect on ramp velocity caused by reduced pressure drop at stall. E_1, 10 v; E_2, 0; E_3, 50 v.

Figure 8. - Continued. Analog solutions of peak holding control.

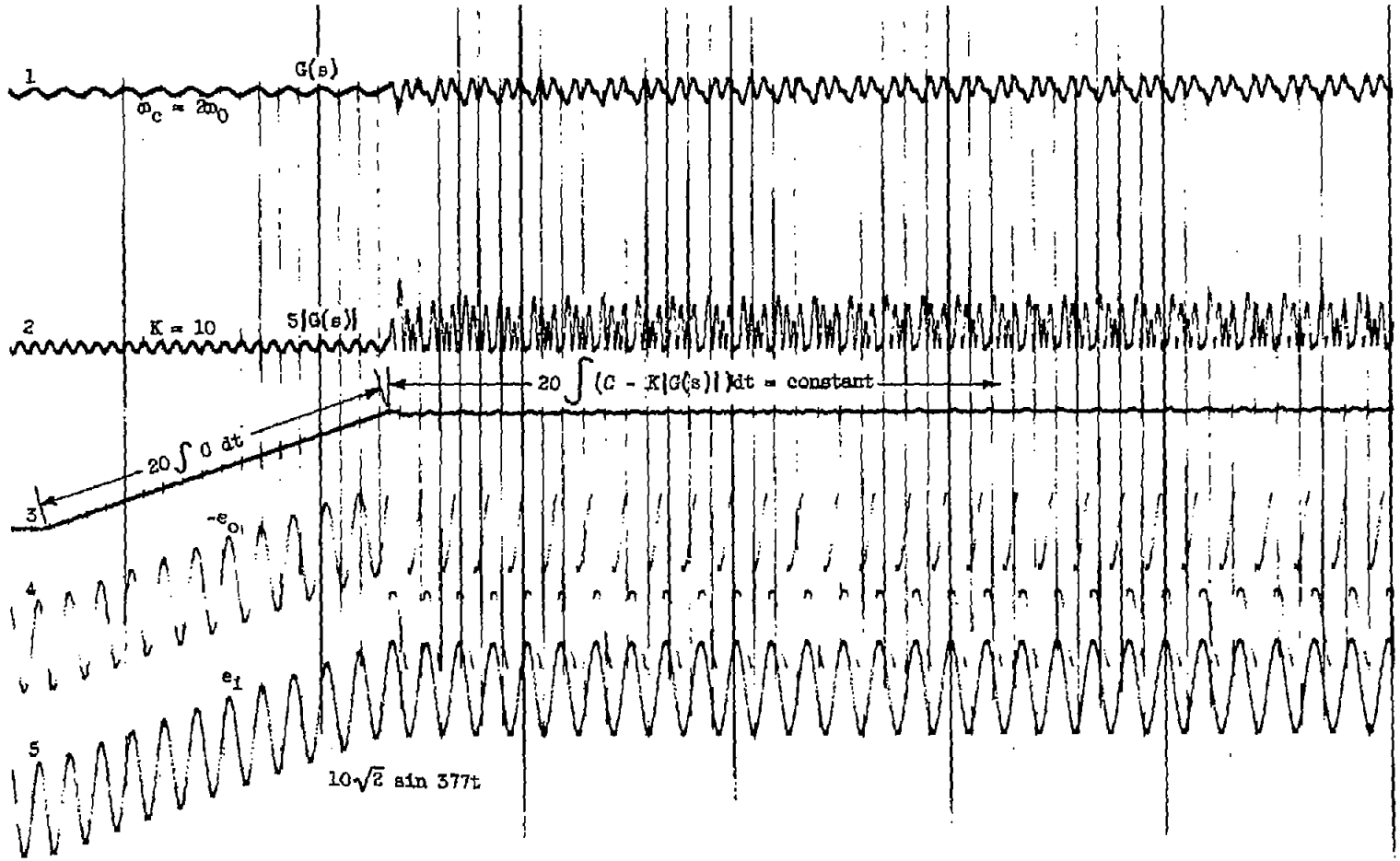

(f) Effect on stability due to hysteresis. E_1 = 30 v, E_2, 25 v; E_3, 50 v.

Figure 8. - Continued. Analog solutions of peak holding control.

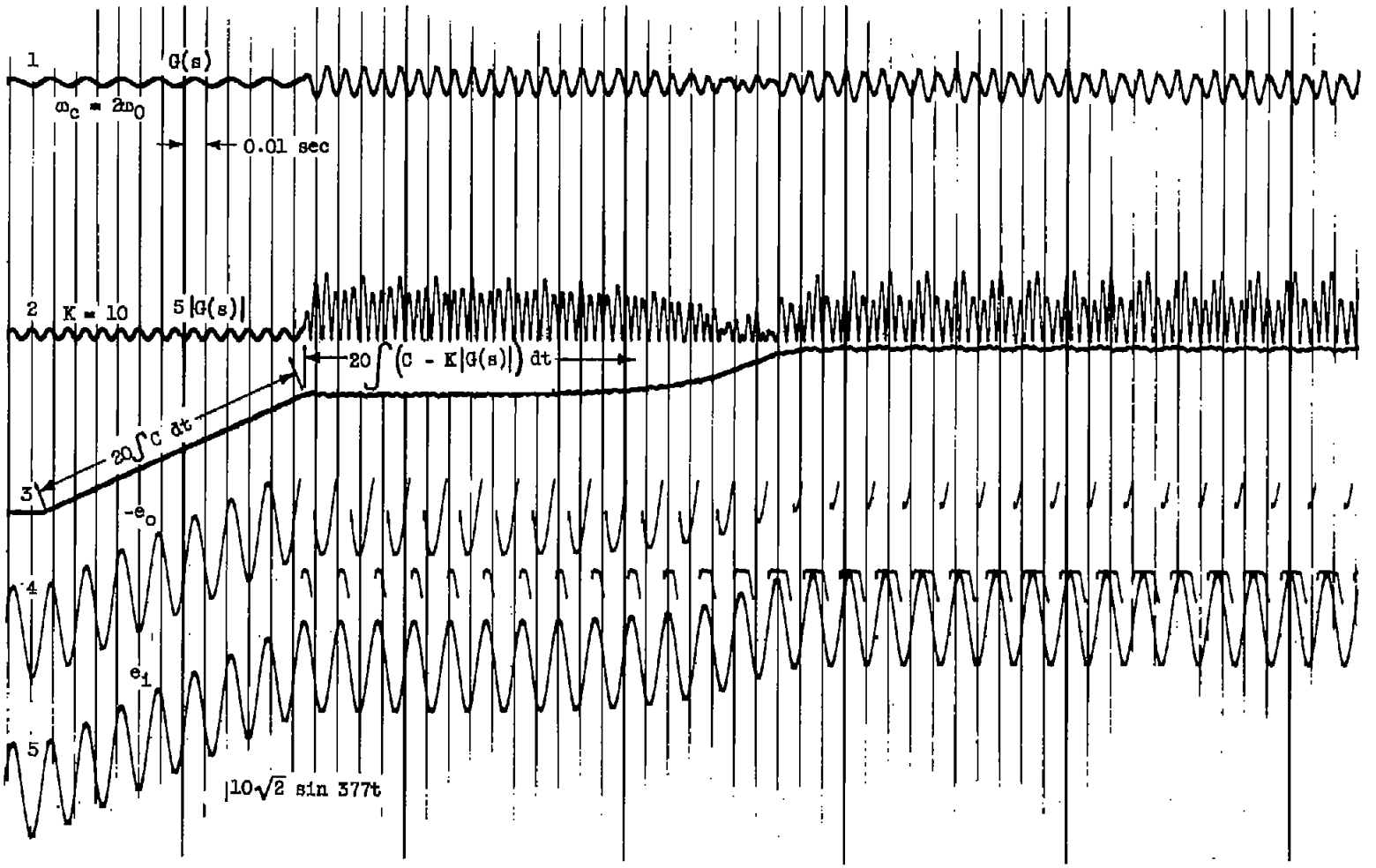

(g) Existence of two stable points. E_1, 30 v; E_2, 10 v; E_3, 50 v.

Figure 8. - Concluded. Analog solutions of peak holding control.

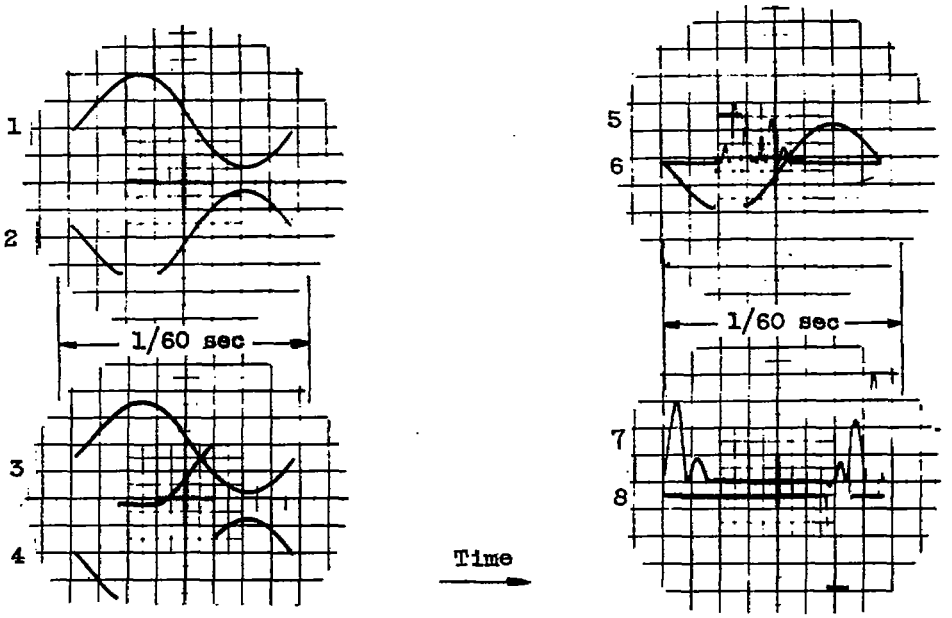

(1) Simulator input
(2) Simulator output, no hysteresis
(3) Simulator input
(4) Simulator output, hysteresis
(5) Absolute value, filter output
(6) Simulator output, no hysteresis
(7) Absolute value, filter output
(8) Simulator output, 2nd stable point

Figure 9. - Simulator and filter outputs at stable conditions.

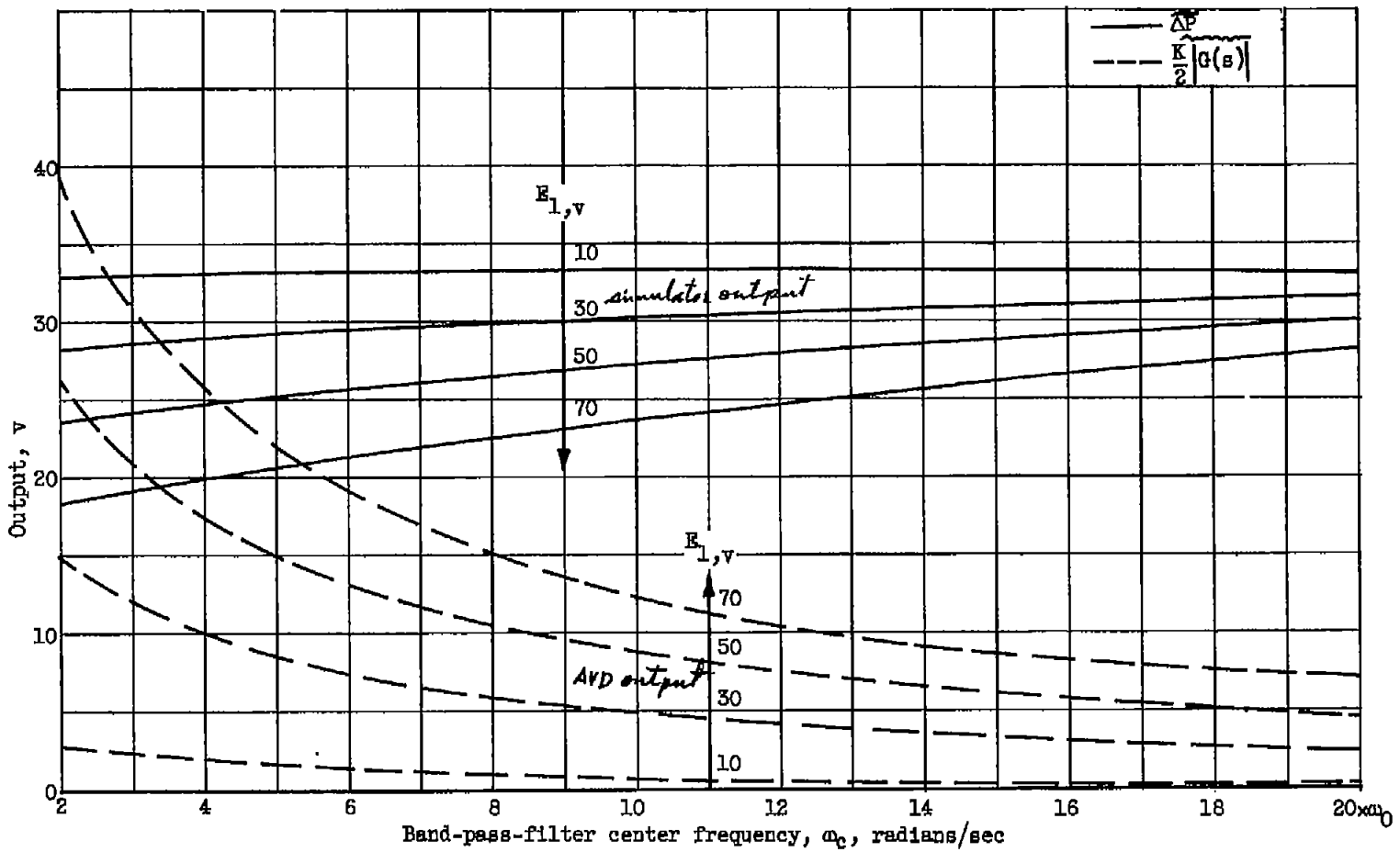

(a) Variation of band-pass-filter center frequency ω_c. Minimum band width. Hysteresis, E_2 = 0 v.

Figure 10. - Effect of filter parameters on measured system variables. Fundamental frequency, $\omega_0 = 120\pi$; pressure at stall, E_3 = 50 v; sinusoidal amplitude, A = $10\sqrt{2}$ v; gain in feedback path, K = 20.

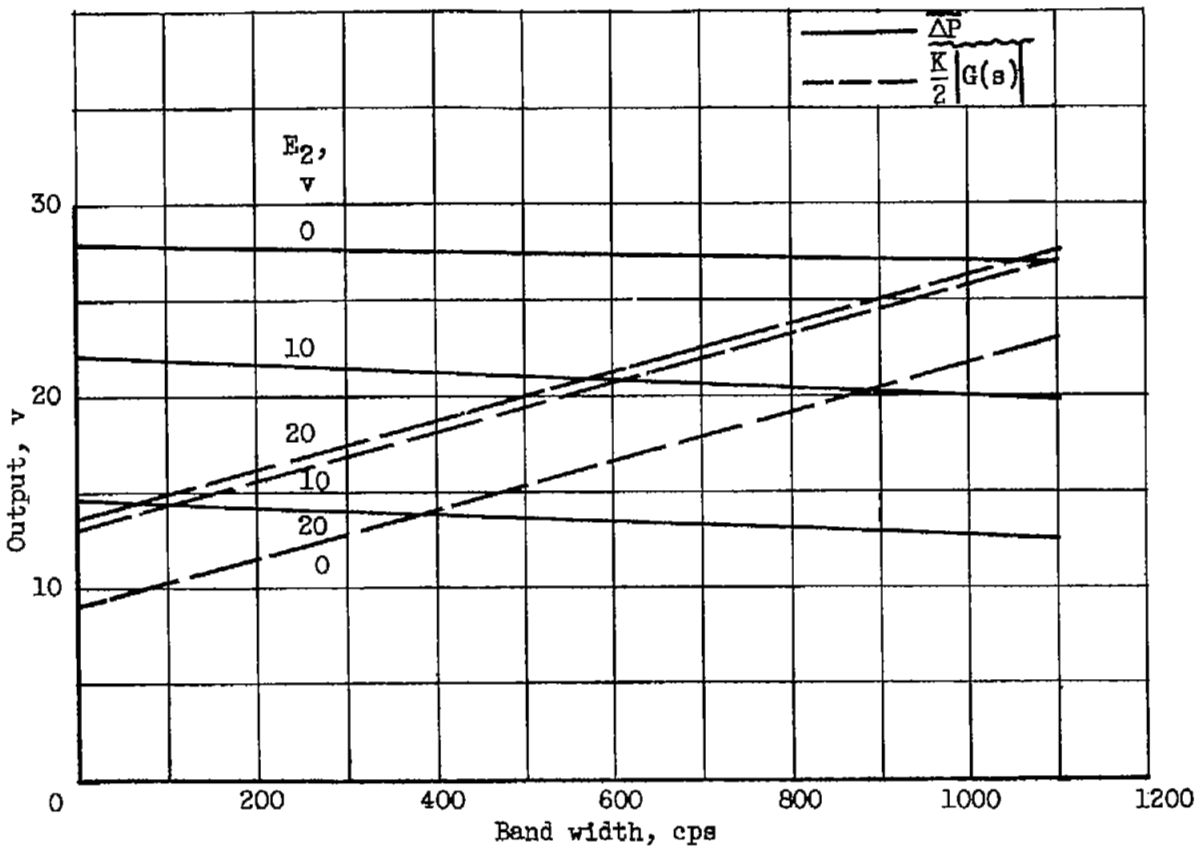

(b) Variation of filter band width. Center frequency $\omega_c = 10\omega_0$. Pressure drop at stall, $E_1 = 50$ v.

Figure 10. - Concluded. - Effect of filter parameters on measured system variables. Fundamental frequency, $\omega_0 = 120\pi$; pressure at stall, $E_3 = 50$ v; sinusoidal amplitude, $A = 10\sqrt{2}$ v; gain in feedback path, $K = 20$.

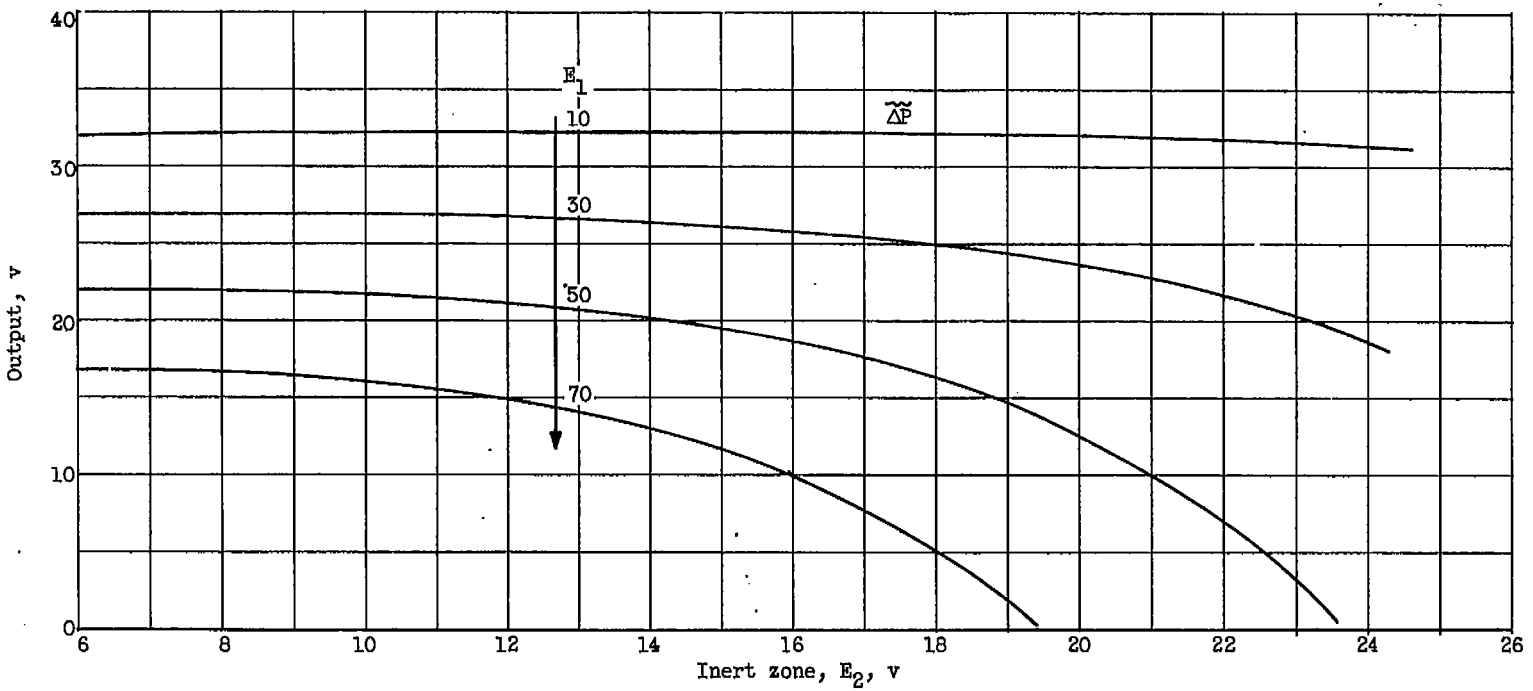

(a) Average output pressure.

Figure 11. - Effect of hysteresis on measured system variables. Fundamental frequency, $\omega_0 = 120\pi$; pressure at stall, $E_3 = 50$ v; sinusoidal amplitude, $A = 10\sqrt{2}$ v; gain in feedback path, $K = 20$; filter center frequency, $\omega_c = 10\omega_0$; minimum band width.

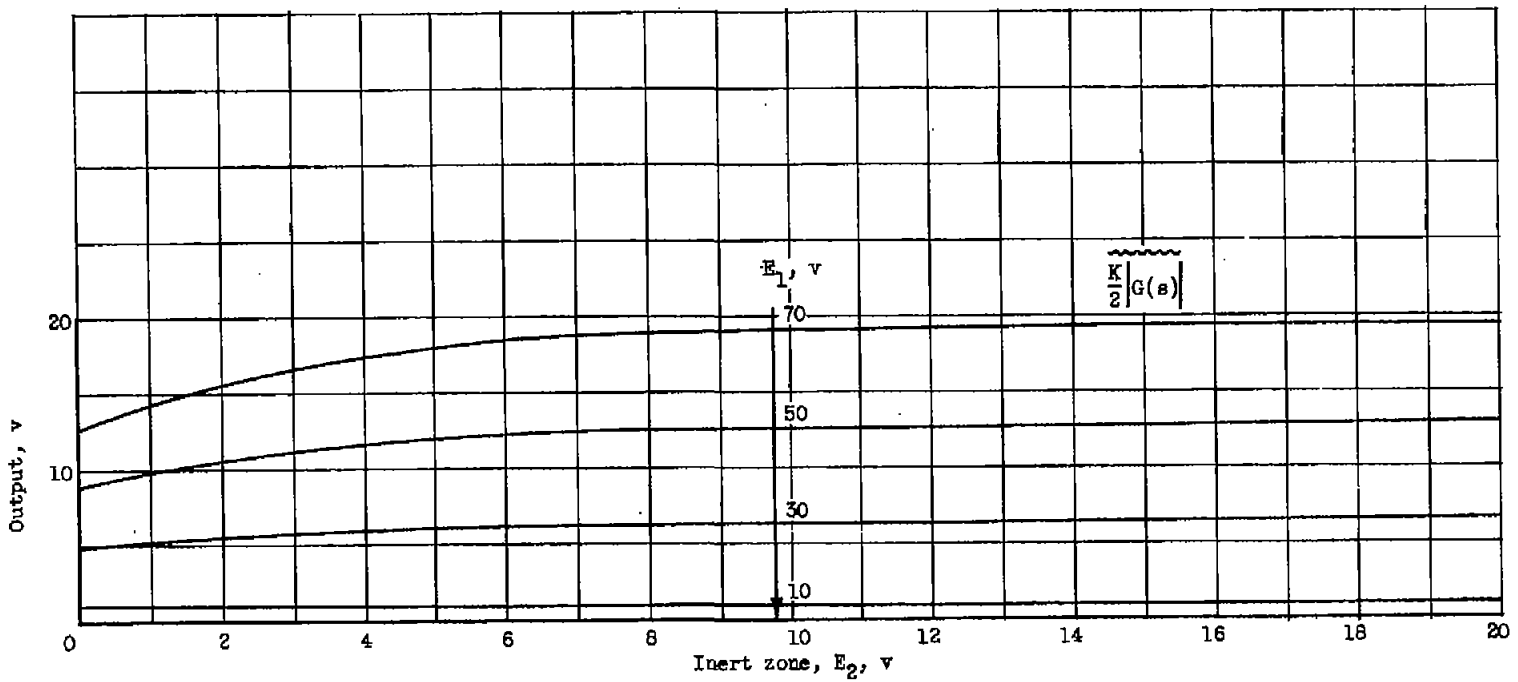

(b) Average absolute value of filter output.

Figure 11. - Concluded. Effect of hysteresis on measured system variables. Fundamental frequency, $\omega_0 = 120\pi$; pressure at stall, $E_3 = 50$ v; sinusoidal amplitude, $A = 10\sqrt{2}$ v; gain in feedback path, $K = 20$; filter center frequency, $\omega_c = 10\omega_0$; minimum band width.

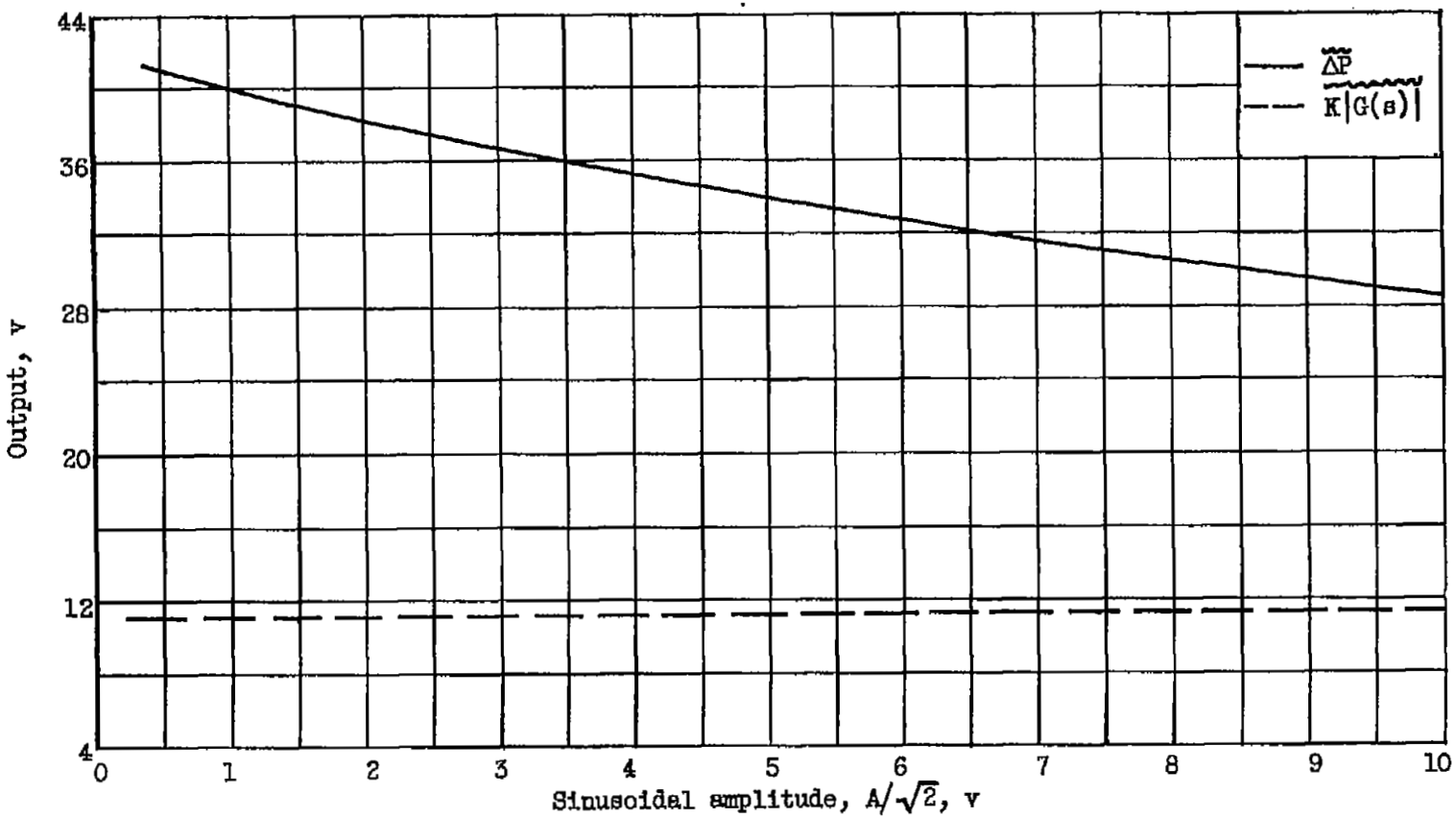

Figure 12. - Effect of sinusoidal amplitude on measured system variables. Fundamental frequency, $\omega_0 = 120\pi$; pressure drop at stall, $E_1 = 50$ v; hysteresis, $E_2 = 0$; pressure at stall, $E_3 = 50$ v; gain in feedback path, $K = 5$; filter center frequency, $\omega_c = 10\omega_0$; filter band width, $2\omega_0$ to $20\omega_0$.

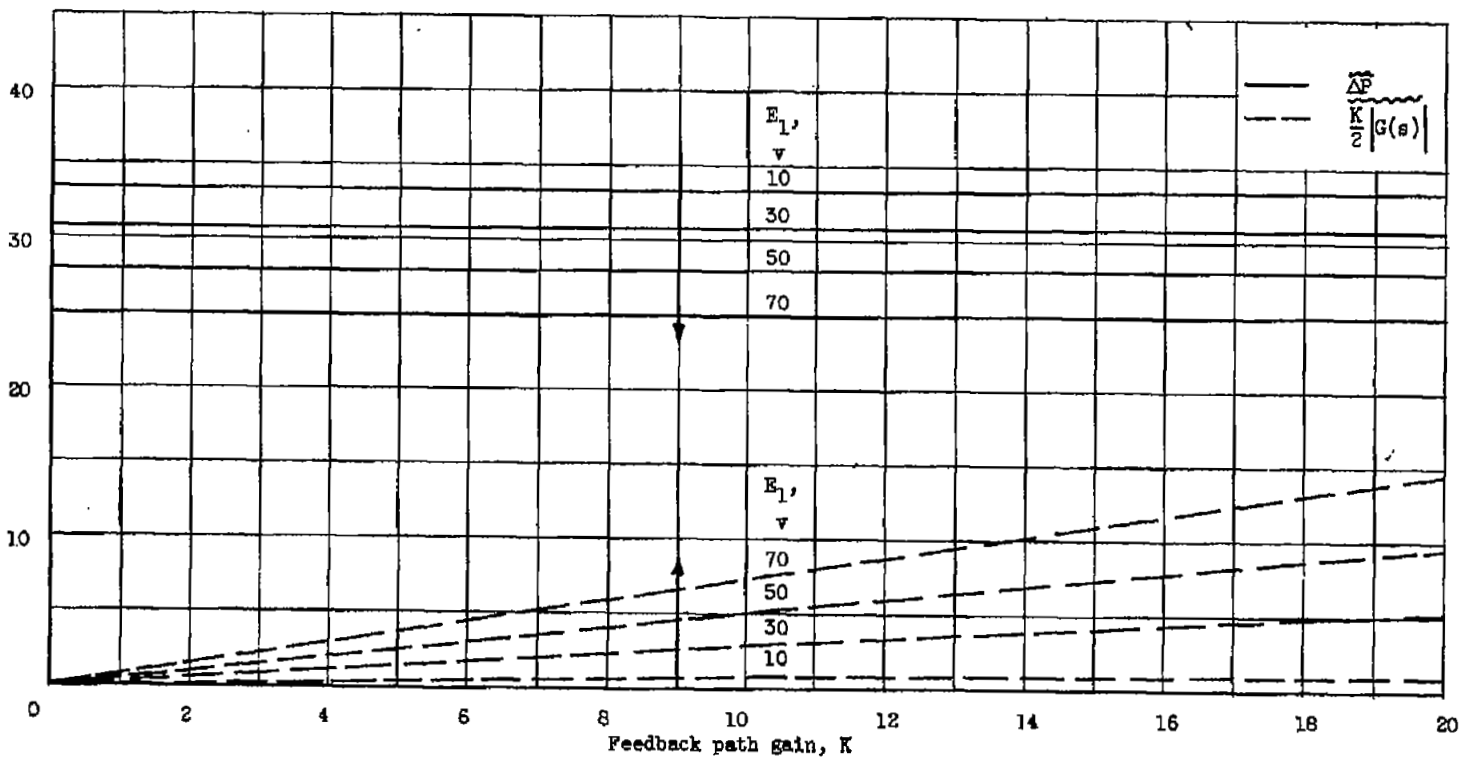

Figure 13. - Effect of feedback path gain on measured system variables. Fundamental frequency, $\omega_0 = 120\pi$; hysteresis, $E_2 = 0$; pressure at stall, $E_3 = 50$ v; sinusoidal amplitude, $A = 10\sqrt{2}$ v; filter center frequency, $\omega_c = 10\omega_0$; minimum filter band width.

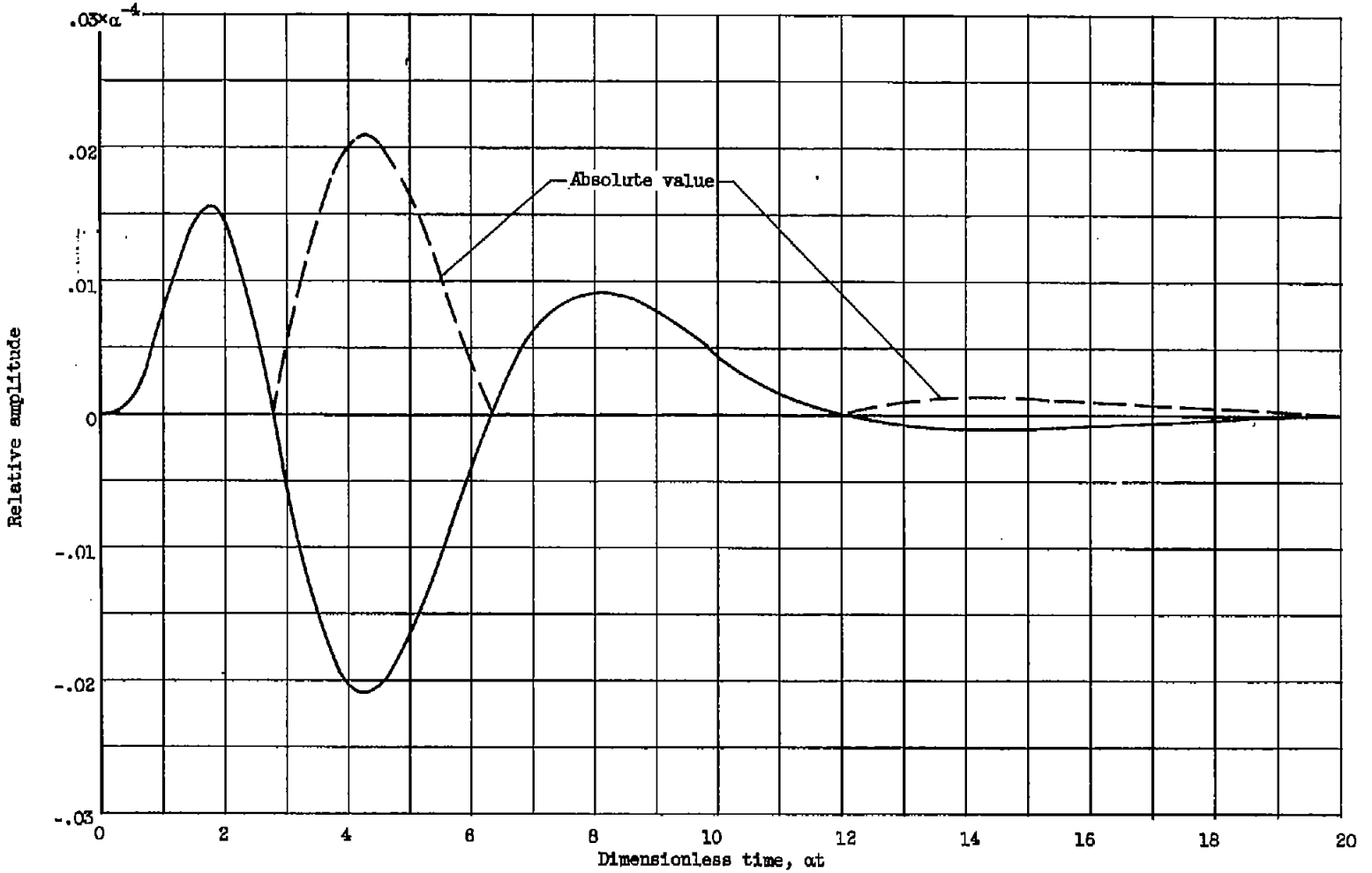

$$f(t) = \mathcal{L}^{-1}\left(\frac{\alpha^4 s^3}{(s+\alpha)^8}\right) = \frac{\alpha^4 t^4\, e^{-\alpha t}}{41}\left[1 - \frac{3}{5}(\alpha t) + \frac{1}{10}(\alpha t)^2 - \frac{1}{210}(\alpha t)^3\right]$$

Figure 14. - Indicial response of filter.

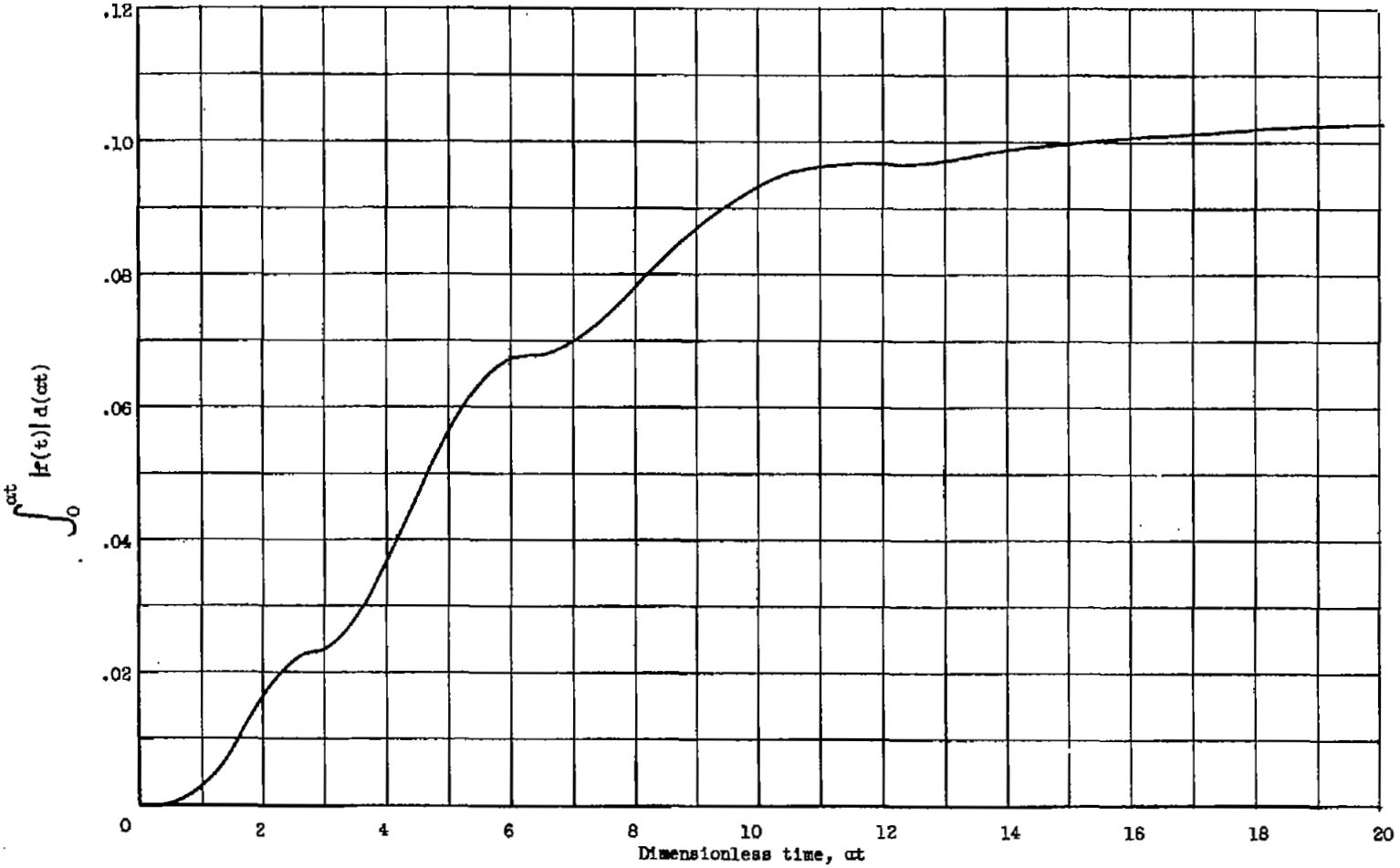

Figure 15. - Time integral of absolute value of filter indicial response.

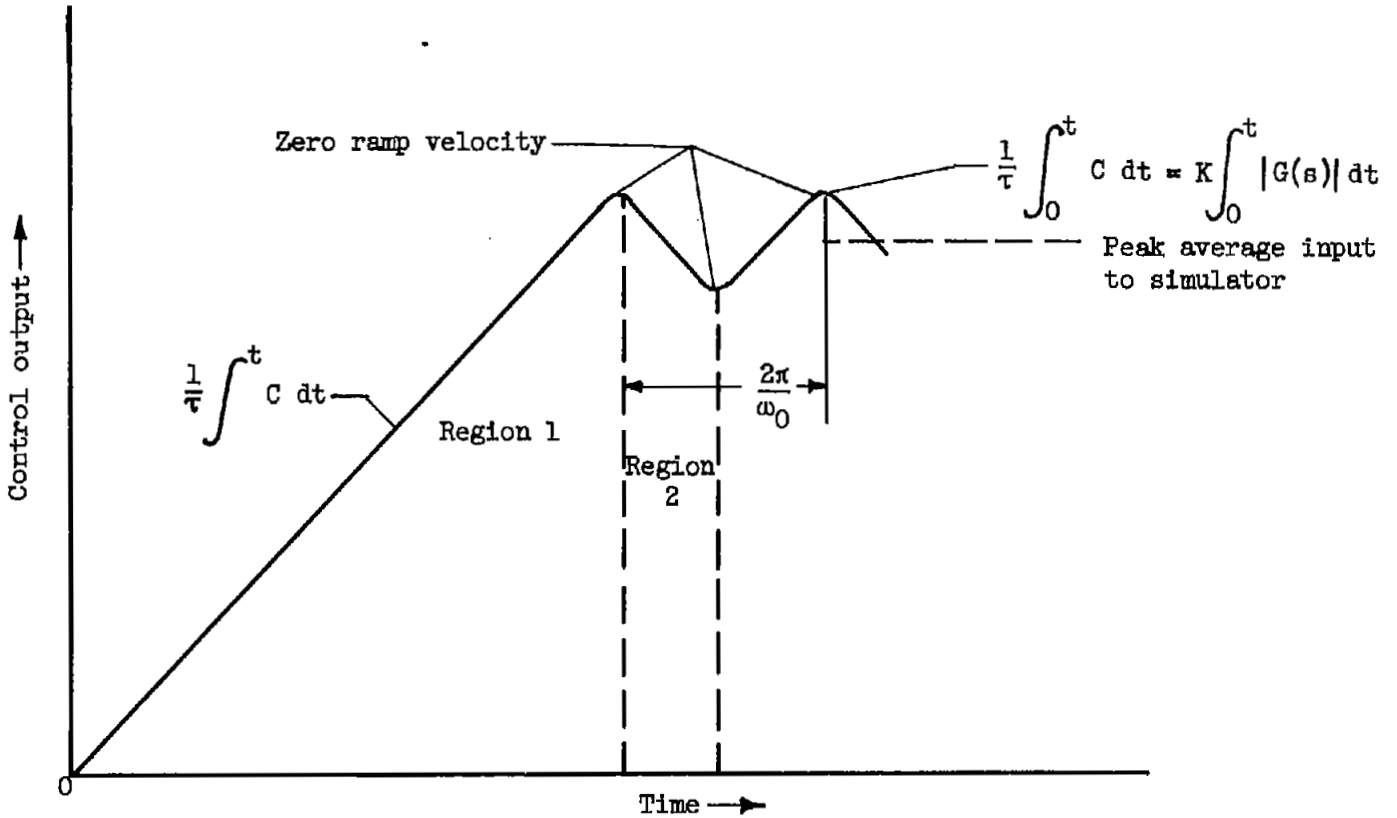

Figure 16. - Theoretical behavior of peak holding control.

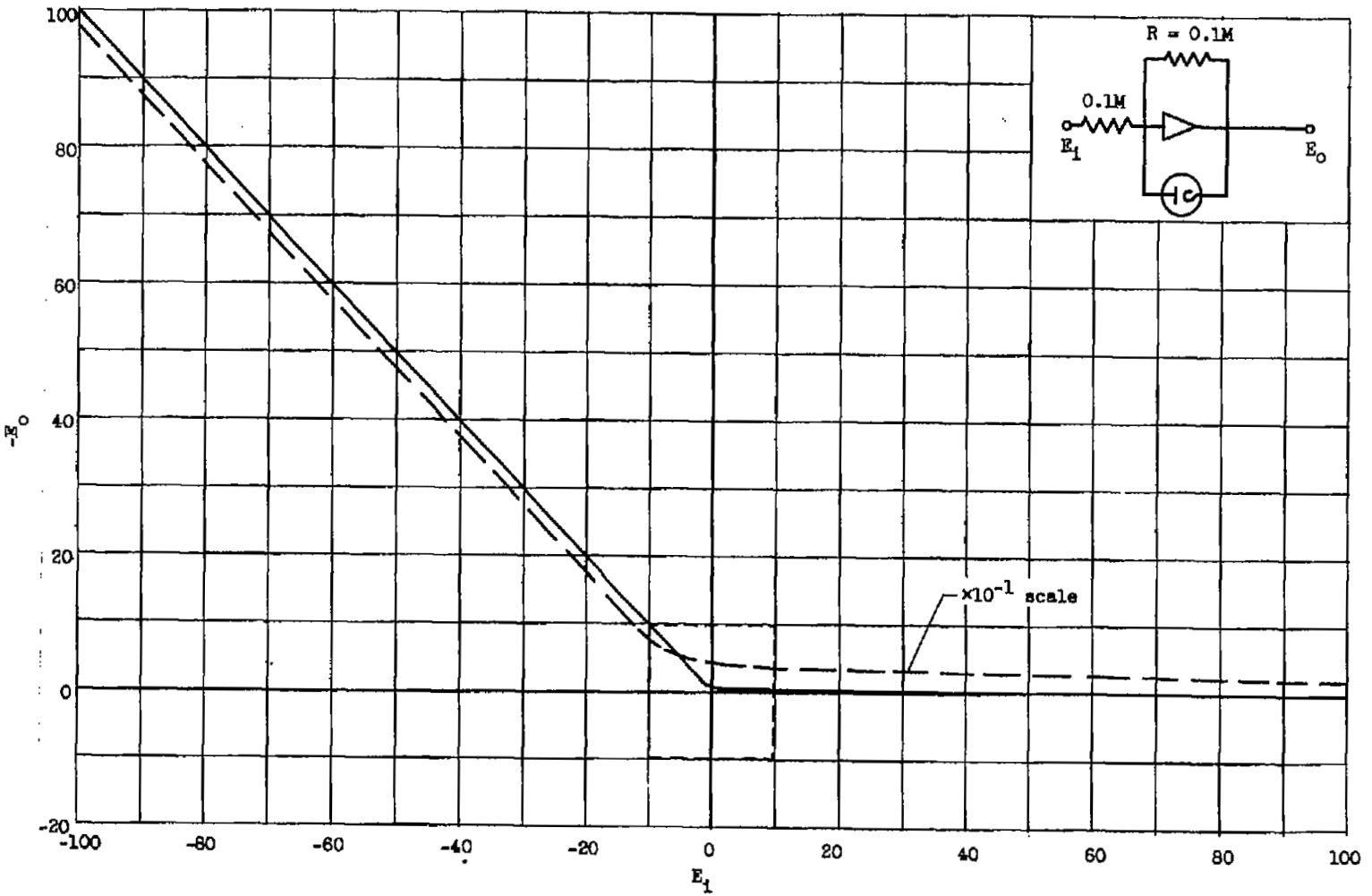

Figure 17. - Limiter characteristics, showing error introduced by finite diode impedance.

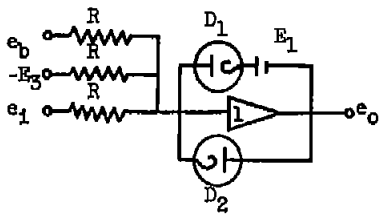

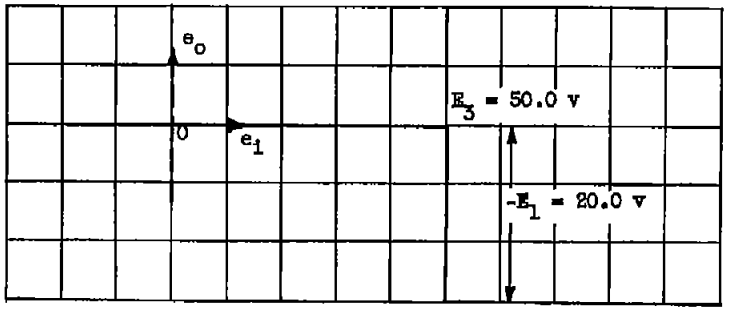

(a) Comparator.

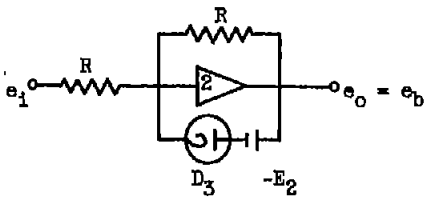

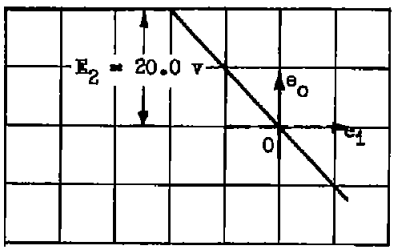

(b) Series output limiter.

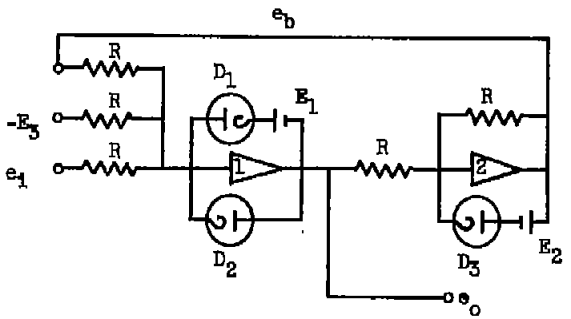

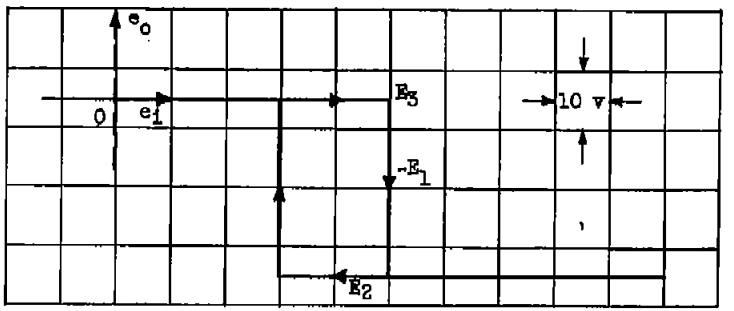

(c) Bistable multivibrator.

Figure 18. - Modified bistable multivibrator possessing a hysteresis loop whose position and area can be independently adjusted. R, 0.1 megohm.

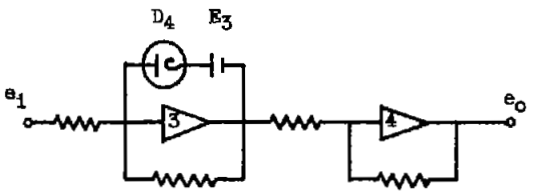

(a) Series output limiter.

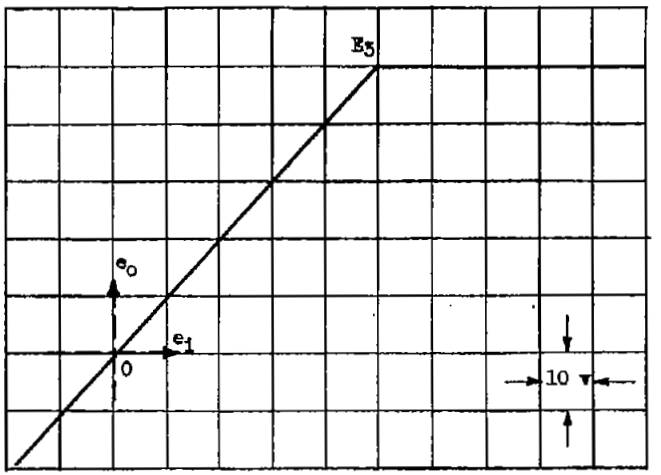

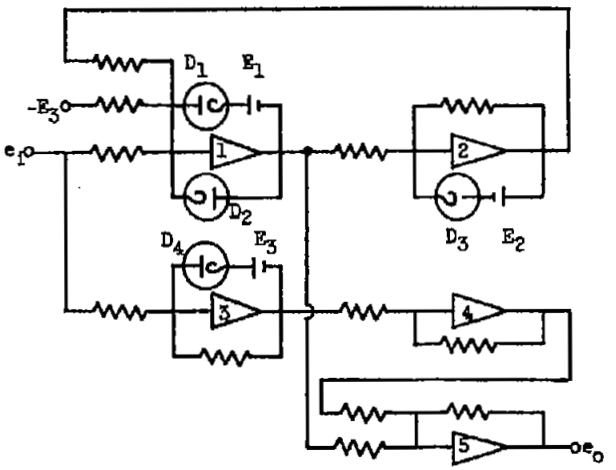

(b) Function generator.

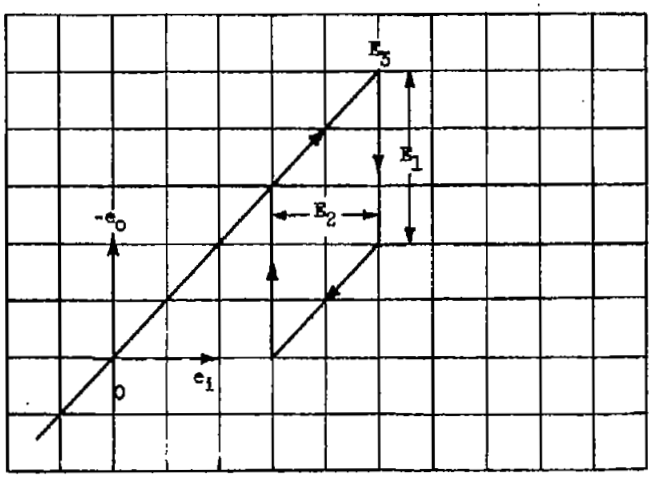

Figure 19. - Theoretical function generator that simulates compressor behavior at stall at constant-speed conditions.

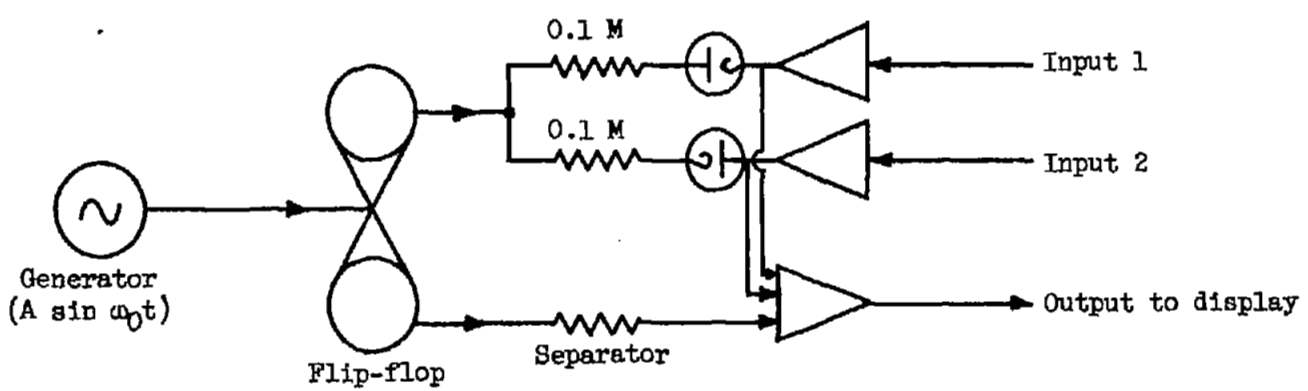

Figure 20. - Arrangement for independent gain adjustment and simultaneous display of two solutions.